Dissolving Nonionic Surfactants in CO₂ to Improve Oil Recovery in Unconventional Reservoirs via Wettability Alteration

Lauren C. Burrows ^a, Foad Haeri ^a, Deepak Tapriyal ^a, Sean Sanguinito ^a, Parth G. Shah ^b, Peter Lemaire ^b, Dustin Crandall ^c, Robert M. Enick ^{b*}, Angela Goodman ^{d*}

- ^a NETL Support Contractor, 626 Cochrans Mill Road, P.O. Box 10940, Pittsburgh, PA 15236, USA.
- ^b University of Pittsburgh, Department of Chemical and Petroleum Engineering, 940 Benedum Hall, Pittsburgh, PA 15261, USA.
- ^c United States Department of Energy, National Energy Technology Laboratory, 3610 Collins Ferry Rd, Morgantown, WV 26505, USA.
- ^d United States Department of Energy, National Energy Technology Laboratory, 626 Cochrans Mill Road, P.O. Box 10940, Pittsburgh, PA 15236, USA.

KEYWORDS: CO₂-soluble surfactants, shale, oil recovery, wettability alteration

ABSTRACT: CO₂ injection is a promising method for enhanced oil recovery (EOR) in unconventional shale reservoirs. In this work, we postulate that CO₂ EOR may be improved by the dissolution of surfactants into CO₂. Although CO₂ is a relatively good solvent for oil, we show that CO₂ and Eagle Ford oil are immiscible at compositions above 70 wt% CO₂, even at pressures as high as 62 MPa. The presence of a CO₂-oil interface at reservoir conditions indicates that the addition of a surfactant has the potential to improve oil recovery—via wettability alteration from oil-wet to CO₂-wet, CO₂-oil interfacial tension (IFT) reduction, or both. Three nonionic surfactants (branched tridecyl ethoxylate Indorama SURFONIC TDA-9, branched nonylphenol ethoxylate Indorama SURFONIC* N-100, and linear dodecyl ethoxylate Indorama SURFONIC* L12-6) were evaluated for CO₂-solubility, shale wettability alteration, effect on CO₂-oil IFT, ability to generate CO₂-oil foams, and ability to increase oil extraction from Eagle Ford, Mancos, and Bakken shale cores. Each surfactant dissolved in CO₂ up to 1 wt% at pressures and temperatures commensurate with CO2 EOR. CO2-dissolved surfactants did not significantly affect CO₂-oil IFT or generate CO₂-oil foams, but they did induce a dramatic change in the contact angle of an oil droplet on an oil-aged shale chip in CO₂ from strongly oil-wet (11°) toward intermediate CO₂-oil wettability (82°) (at 80 °C, 27.6 MPa). The branched tridecyl ethoxylated surfactant, SURFONIC® TDA-9, afforded the highest oil recovery in core soaking experiments—75%, compared to 71% by pure CO₂. Analysis of oil extracts by gas chromatography revealed that heavier oil components were produced when the surfactant was added to CO₂. These results indicate that CO₂-dissolved surfactants may increase oil recovery from shale by wettability alteration from oil-wet toward CO₂-wet.

1. INTRODUCTION

Meeting the world's growing energy needs in the face of climate change is one of the greatest scientific challenges of our time. In the United States, domestic shale oil provides a critical supply of energy,¹ but the environmental damage inflicted by hydraulic fracturing and fossil fuel emissions is problematic. Domestic energy production has become increasingly desirable,² but because of the tight nature of U.S. shale reservoirs, approximately 90% of the oil in these reservoirs is inaccessible by the current hydraulic fracturing technology.³ New wells must be drilled and fractured rapidly to maintain oil production, imposing greater environmental costs. Therefore, new methods are

needed to safely access trapped oil in already-fractured shale wells.

One strategy for producing oil from already-fractured shale wells involves injecting oil-miscible gases such as CO₂, ethane, propane, nitrogen, or natural gas to extract the remaining oil.^{3,4,5,6,7,8,9,10,11,12,13} Of all the gases tested, CO₂ has demonstrated several advantages. CO₂ increases oil extraction by a variety of mechanisms including diffusion, vaporization, oil swelling, oil viscosity reduction, pressure support, CO₂-oil interfacial tension (IFT) reduction, solution gas drive and relative permeability hysteresis.³ Furthermore, the use of CO₂ as an enhanced oil recovery (EOR) fluid has the potential to reduce the carbon intensity of the hydrocarbons produced during fracturing. If

^{*}Email: rme@pitt.edu, angela.goodman@netl.doe.gov

anthropogenic CO₂ is injected, some of the CO₂ will be trapped in the subsurface, ^{14, 15} offsetting the CO₂ emissions that result from combustion of the produced hydrocarbons. ^{16, 17, 18, 19}

Given the environmental advantages of using CO₂ as an EOR fluid, we set out to further improve the efficacy of CO₂ for extracting oil from shale. We proposed to do this by dissolving small amounts of surfactants directly in CO₂.²⁰, ^{21, 22} Surfactants dissolved in water have been shown to improve oil recovery from shale by changing shale wettability toward water-wet or reducing the IFT between oil and water.23,24 In this study, surfactants were dissolved in CO2 to attain analogous shifts in wettability or IFT. We chose to add surfactants to the CO₂ phase to avoid additional water injection. Although ionic surfactants are essentially insoluble in CO₂, 25 nonionic surfactants have been previously dissolved in CO2 to generate CO2-in-water foams in conventional reservoirs. 26, 27, 28, 29, 30, 31, 32 Weak electrostatic interactions resulting from the presence of an electropositive carbon atom and two electronegative oxygen atoms enable oxygen-rich surfactants to dissolve in liquid or supercritical CO₂.

The nonionic surfactants selected for this study all contain a hydrocarbon segment and a poly(ethylene oxide) (PEO) segment. These surfactants are similar in structure to those previously employed to generate CO₂-in-brine foams, but the hydrocarbon and PEO segments serve different purposes. In previous applications where the two liquid phases were CO₂ and brine, the hydrocarbon segment was hydrophobic while the PEO segment was hydrophilic. In that case, the PEO groups were longer (9 to 15 EO units) to enable the surfactant to partition into the brine phase in the subsurface. Here, where the two fluid phases are CO₂ and oil, the hydrocarbon segment is oil-philic and the PEO segment is oil-phobic. Brine solubility is not needed, so PEO segments are designed to be long enough to induce wettability changes,33 without being so long that they reduce CO₂ solubility (6-10 units).

Because the IFT between CO₂ and oil is already low at reservoir temperatures and pressures, 34, 35, 36, 37 and CO2-oil foams are very difficult to generate, 38, 39 we anticipated that wettability alteration of shale from oil-wet to water-wet (or CO₂-wet) would be the key mechanism by which CO₂-dissolved surfactants would improve oil recovery. Shale is oilwet because of the presence of oil-wetting deposits on the shale mineral surface (Figure 1A).40, 41, 42 These deposits cause oil to adhere to the shale, making it more difficult to produce. The oil-wetting deposits are polar, charged or polyaromatic compounds that are insoluble in CO₂. Because we are using nonionic surfactants, these deposits are not likely to be removed by ion pair formation or micellar solubilization mechanisms. Instead, the most likely mechanism for wettability alteration is by surfactant adsorption to the shale surface.33 During CO₂ EOR, as CO₂ soaks into shale fractures and pores, a CO₂-dissolved surfactant can adsorb to the oil-wet shale surface with the alkyl segment of the nonionic surfactants interacting with the oil-wetting deposits via van der Waals forces and the PEO segment of the nonionic surfactant extending outward, rendering the surface more CO₂-wet (and water-wet) (Figure 1B). This change in surface wettability will cause the oil to bead up and be produced more easily.

Because surfactant activity requires the existence of two fluid phases, we began our study by investigating the phase behavior between CO2 and Eagle Ford oil (Table 1, column 1). High-pressure experiments were performed to determine whether the selected surfactants—branched tridecyl ethoxylate Indorama SURFONIC® TDA-9, branched nonylphenol ethoxylate Indorama SURFONIC® N-100, and linear dodecyl ethoxylate Indorama SURFONIC® L12-6 (Figure 2)—were soluble in CO₂ (Table 1, column 2). The mechanism of surfactant activity was investigated through ambient pressure contact angle experiments, followed by high-pressure CO2-oil IFT measurements and foaming experiments. High-pressure, high-temperature contact angle experiments were performed to directly observe whether a CO2-dissloved surfactant could alter the wettability of shale (column 5, a). To our knowledge, this experiment represents the first time that a contact angle measurement of an oil droplet on shale in CO2 has been performed. The ability of CO₂-dissolved surfactants to increase oil recovery was tested via huff-n-puff experiments involving cores both completely immersed in CO2 and CO2+surfactant solutions (column 5, b), and cores confined with a rubber sleeve so that only one end was exposed (column 5, c). The molecular weight distributions of hydrocarbons produced in the confined huff-n-puff experiments were quantified by gas chromatography-mass spectrometry (GC-MS) analysis (column 5, d). Throughout this study, when experiments were limited to one surfactant, the branched tridecyl ethoxylate surfactant, SURFONIC TDA-9° was tested because this surfactant afforded highest oil recoveries in our initial huff-n-puff experiments.

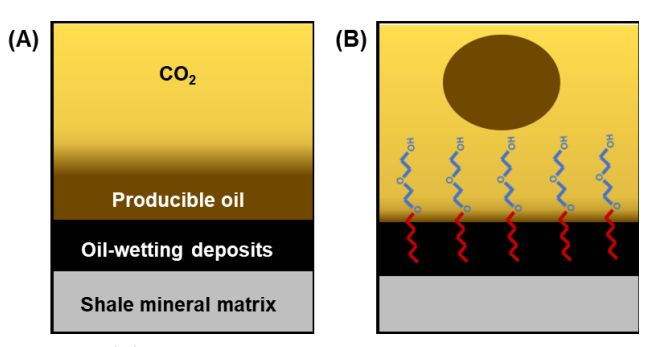


Figure 1. (A) CO₂ EOR without surfactants. CO₂ extracts producible oil from pores and fracture surfaces by diffusion and other mechanisms. Oil-wetting deposits (polar, charged and polyaromatic organic compounds) remain on the shale mineral matrix. (B) CO₂ EOR with surfactants dissolved in the CO₂ phase. Surfactants interact with the oil-wet shale surface and alter it toward CO₂-wet, thereby increasing oil production.

In this work, our goal was to determine whether CO_2 -dissolved surfactants can alter the wettability of shale, and whether that alteration leads to an increased oil recovery in unconventional formations when compared to CO_2 alone. To the best of our knowledge, this work represents the first time that surfactants have been dissolved directly in CO_2 to increase shale oil extraction via wettability alteration.^{43, 44, 45, 46, 47, 48} Others have added surfactants to the

aqueous phase during surfactant-alternating-CO₂ gas (SAG) injection in shale,⁴⁹ pre-soaked cores in aqueous surfactant solutions before CO₂ injection,^{50, 51} co-injected aqueous surfactant solutions with CO₂ to produce foams,⁵² used ethanol as a co-solvent to dissolve ionic and nonionic surfactants in CO₂,^{53, 54, 55} or used high concentrations of CO₂-soluble surfactants (o.5 wt%) to reduce CO₂-oil IFT.⁵⁶ In our current study, no water, brine, or co-solvent is introduced to the shale during the huff-n-puff process; only the injection of a CO₂-surfactant solution is considered. The surfactants used in this study are all commercially-

available, cost approximately \$1-3 per pound, and are anticipated to be effective at concentrations of 0.1 wt% or less.²⁷ Therefore, the surfactant would add approximately \$2-6 to the cost of one ton of CO₂. The injection of CO₂-surfactant solutions has been completed successfully on the field scale for CO₂-foam generation in conventional reservoirs, and the same equipment can be used for CO₂ EOR in unconventional reservoirs.²⁹ Thus, dissolution of surfactants in CO₂ may be an economically and logistically viable strategy for improving CO₂ EOR in unconventional reservoirs.

Table 1. Workflow of experiments in this study. = high pressure (27.6 MPa) and temperature (80 °C) = ambient pressure and temperature												
1		2	3 CO ₂ +	(4	D .	3						
CO ₂ +Oil	Surfactants ^a	CO ₂ + Surfactants	Surfactants + Shale	CO ₂ +Oil+	Surfactants	CO ₂ + Surfactants + Oil + Shale						
Phase		CO ₂ Solubility	Air-Water Contact Angle	(a) IFT Measure- ment	(b) Foam experiment	(a) CO ₂ -Oil Contact Angle	(b) Immersed Core Huff-n-Puff	(c) Confined Core Huff-n-Puff	(d) Oil Analysis GC-MS			
Behavior	TDA-9	х	х	х	х	х	х	х	х			
	N-100	x	x				х					
	112-6	v					v					

^a Surfactants were obtained from Indorama.

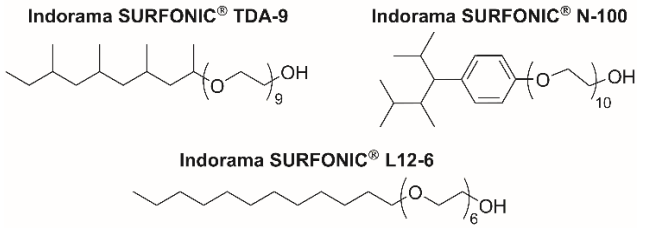


Figure 2. Nonionic ethoxylated alcohol surfactants from Indorama used in this study.

2. EXPERIMENTAL METHODS

2.1 Materials and general methods. Because availability of field cores from oil-producing zones was limited, outcrop cores aged in oil were used in this study. Eagle Ford and Mancos outcrop shale cores were purchased from Kocurek Industries. Bakken cores were obtained from the Bedwell 33-52-1-1H Well in Sheridan County, MT.57 Shale chips (0.25 cm \times 0.76 cm × 0.51 cm) used in contact angle experiments were cut from outcrop Eagle Ford cores. Eagle Ford crude oil was obtained from Continental Resources, Inc. The oil temperature and pressure were not maintained at subsurface conditions, and as such, shorter-chain hydrocarbons (n-C5 and lower) exsolved from solution prior to our analyses. The composition of the Eagle Ford oil used in our experiments is shown in Figure 3. CO₂ (99.9%) was obtained from Butler Gas (Pittsburgh, PA). Nonionic surfactants tridecyl ethoxylate SURFONIC® TDA-9, nonylphenol ethoxylate SURFONIC® N-100, and dodecyl ethoxylate SURFONIC® L12-6 were newly synthesized at Indorama Oxides and Derivatives and immediately shipped to the University of Pittsburgh prior to our experiments. All three surfactants were pure liquids (>99%) containing no solvents or other additives. The pour points of these surfactants are 18 °C, 3 °C, and 10 °C, respectively. Throughout our study, operating conditions of 27.6 MPa and 80 °C were selected as representative of the low temperature range associated with unconventional formations targeted for CO₂ EOR.³ Connate water was not included in the huff-n-puff experiments due to the inability of our oil recovery measurements, which were based on the weight of the core after each "puff", to distinguish between water and oil production. Connate water was omitted from contact angle experiments to maintain consistency with the huff-n-puff experiments. ⁵⁸

2.2. CO₂-Oil pressure-composition. A pressure-composition (Px) diagram was generated for mixtures of CO2 and Eagle Ford crude oil at a single temperature (80 °C). A series of isothermal compression and expansions of CO₂-oil mixtures of known overall composition were performed using the variable-volume view cell apparatus shown in Figure 4. For each experiment at a given CO₂-oil composition, components were injected into a thick-walled Pyrex sample tube with a sliding piston in the following manner. First, a specified mass of oil was added to the tube above the piston at room temperature (rt, 22 °C). The tube was then inserted into a high-pressure, variable-volume (10-100 mL), windowed, invertible phase behavior cell housed within a temperature-controlled air bath (-20 °C to 180 °C) (Schlumberger JEFRI cell, rated to 180 °C and 69 MPa). The lid to the phase behavior cell, which is equipped with a magnetically-driven slotted-fin impeller, was closed. The transparent overburden fluid (low viscosity silicone oil, polydimethylsiloxane, PDMS) was then pumped into the bottom of the phase behavior cell to compress the oil to 13.8 MPa. The overburden fluid filled the narrow gap between the outer wall of the tube and the inner wall of the phase behavior cell, and the space below the sliding piston within the tube. Next, high-pressure liquid CO₂ was pumped into the tubing leading to the valve at the top of the phase behavior cell until the pressure of the liquid CO₂ in the tubing was the same as the pressure of the oil in the cell (13.8 MPa). The valve at the top of the phase behavior cell was opened. Using the computer-controlled pump system, a precise volume of CO₂ was pumped

into the sample cell at the same volumetric rate that overburden fluid was withdrawn from the phase behavior cell, resulting in an isothermal, isobaric, addition of CO₂ into the Pyrex tube. The mass of CO₂ introduced to the sample tube is the product of CO2 density at 23 °C and 13.8 MPa and the volume of CO₂ pumped into the cell. Once the desired amount of CO₂ was added to the cell, the valve at the top of the cell was closed, thereby isolating the mixture of known overall composition.

The cell was then heated to 80 °C by a circulating air bath. The mixture was stirred (2,000 rpm) while being compressed to 62 MPa (the operational pressure limit of the cell) via the injection of overburden fluid into the phase behavior cell. At lower proportions of CO₂ (<38%), this procedure resulted in the mixture forming a single liquid phase. The sample volume was then slowly expanded to decrease the pressure. The pressure at which the first bubble of vapor appeared is the bubble point pressure for that composition. Further expansion resulted in an increasing proportion of vapor. The volume fraction of oil-rich liquid phase relative to the total mixture was measured using the ruler on the side of the window.

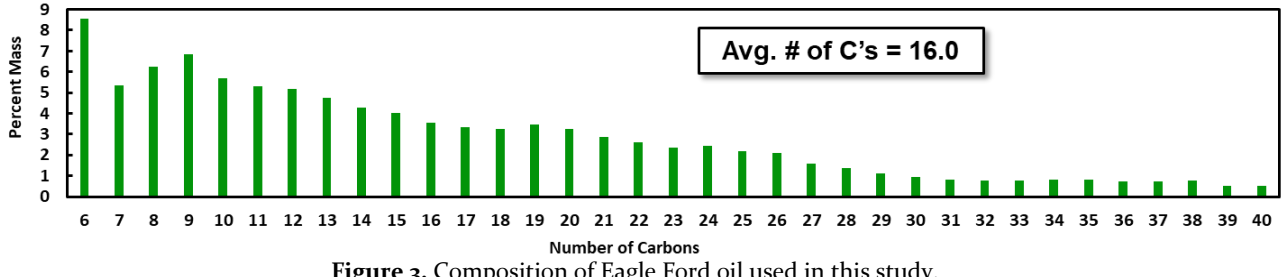


Figure 3. Composition of Eagle Ford oil used in this study.

- **A** Boundary of Air Bath
- **B** Cell Body
- © Window
- Ruler
- Thick-Walled Pyrex Tube
- Magnetically-Driven Impeller
- Sliding Piston and O-Ring
- (II) PDMS Overburden Fluid

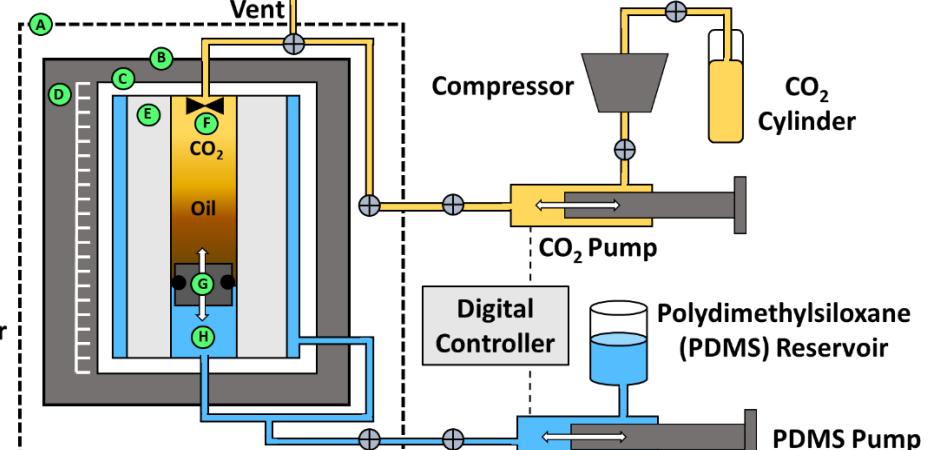


Figure 4. Variable-volume view cell apparatus used for observing CO₂-oil phase behavior.

For mixtures that contained higher proportions of CO₂ (>38%), slow expansion of the single-phase mixture led to the formation of a fine mist of oil-rich droplets. The pressure at which the first droplets appeared is the cloud point for that composition. Further expansion led to an increasing proportion of the oil-rich liquid phase. At highest proportions of CO₂ (>70%), the mixture did not form a single phase when compressed to 62 MPa. Nonetheless, the relative volumes of the oil-rich liquid phase and the CO₂-rich fluid phase were determined as the sample volume was expanded.

2.3. Surfactant solubility measurements. The solubilities of the surfactants in CO₂ were determined using a visual, non-sampling method that is described in our previous publications.^{27, 28, 59} The experiment was performed in the same windowed, variable-volume view cell as described in the previous section (Figure 4). Surfactant solubility was determined as soon as the newly-manufactured surfactants were received. The surfactant and liquid CO₂ were injected into the cylindrical sample volume above the sliding piston. The contents were compressed to 62 MPa and mixed for 30 min using a magnetically-driven slotted-fin impeller spinning at 2,000 rpm. The impeller was stopped, and the entire cylindrical volume of the

cell was inspected to verify that a single, transparent fluid phase was achieved. Then, the single-phase cell volume was expanded slowly until a second phase first appeared in the form of a cloud point of surfactant-rich droplets that caused the entire phase volume to be opaque. The pressure was further reduced below the cloud point to verify that an increasing amount of the second phase came out of solution. This procedure was repeated at least five times and the average value of the cloud points was determined. A phase boundary curve was constructed by adding CO2 to the cell to change the composi-

In addition to their solubilities in CO₂, the solubilities of each surfactant in water, synthetic Eagle Ford brine, and Eagle Ford oil were measured at ambient pressure at rt and 77 °C. The synthetic Eagle Ford brine contained 3.15 wt% NaCl, o.86 wt% CaCl₂·2H₂O, o.20 wt% MgCl₂·6H₂O, o.07 wt% NaHCO₃, 0.06 wt% NaNH₄, 0.02 wt% KCl, and 0.01 wt% Na₂SO₄, in deionized water. 60 For each measurement, known masses of surfactant and fluid (water, brine, or oil) were combined in a 20 ml vial containing a small magnetic stir bar. The vials were capped and placed on a stir plate either at rt or in a temperature-controlled oil bath (77 °C). After one hour of stirring, the mixtures were visually inspected. If the mixture formed a single transparent phase, the surfactant was considered to be soluble in the liquid at that concentration. This procedure was repeated at 1, 2, 3, 4 and 5 wt% surfactant, and at higher concentrations in increments of 5 wt% up to 95 wt%.

2.4. Ambient pressure shale-water-air contact angle measurements. The ability of surfactants to alter the wettability of shale was first investigated at ambient pressure through contact angle measurements using the sessile drop method. New Eagle Ford outcrop shale chips were used in each experiment. We chose to use deionized water in the absence of salts to focus on the wettability alteration by surfactants. Future tests related to possible field trials will be performed with hypersaline brines representative of the shale formation. Resources were not available for conducting contact angle measurements for a series of single minerals. The use of multi-mineral rock samples was performed because the contact angle measurement can be considered to qualitatively represent the fluid-shale interaction over many single mineral pores that occur in a formation such as the Eagle Ford.

In all contact angle measurements, a droplet of deionized water (8-9 $\mu L)$ was placed on a shale chip in air using a microsyringe at ambient pressure and temperature. The droplet was allowed to stabilize, and the contact angle was measured at the water-air-rock contact point through the water phase with an Attension Theta Optical Tensiometer. Measurements were repeated at least three times at different points on the samples and the average values reported.

Eagle Ford outcrop shale chips were cleaned for 5 min using a Harrick Plasma Cleaner (Model PDC-32G) at medium radio frequency level with air as the carrier gas. The original wettabilities of the cleaned shale chips were determined (Figure 5A). Water spread on the clean shale chips and a contact angle of 8° was measured. Then, the shale chips were placed in a closed container of Eagle Ford oil in an oven (80 °C) for at least two weeks. The chip was removed from the container, excess oil wiped off, and the contact angle was re-measured. The oilaged shale chip was confirmed to be oil-wet (contact angle of $117 \pm 5^{\circ}$). The first time this aging process was performed, the shale chip was removed from the oil every other day and the contact angle measured. After two weeks, no further changes in contact angle were observed. Thus, we determined that two weeks was the optimal aging period for shale chips. The effect of aqueous solutions of the three selected surfactants on shale wettability was tested. Solutions of each surfactant-Indorama SURFONIC® TDA-9, N-100, and L12-6 (0.1 wt%)—were prepared in deionized water. An oil-wet shale chip was placed in a beaker containing aqueous surfactant solution (10 mL) at rt. After 24 h, the chip was removed from the solution and wiped with a Kimwipe. The contact angle of a droplet of deionized water on the shale surface was then measured. Measurements were made daily until no further change in wettability was evident.

The effect of pure CO_2 on shale wettability was tested (Figure 5B). A clean shale chip was aged in oil. The oil-aged shale chip was suspended with a wire in the middle of a 15-mL pressure cell housed within an oven. CO_2 (10 g) was added to the cell and pressurized to 27.6 MPa using an ISCO pump. The cell was heated to 80 °C, and the chip was allowed to soak for 16 h. The cell was slowly depressurized and cooled. The sample was removed from the cell and the contact angle of a water droplet on the shale chip in air was measured at ambient pressure and temperature.

The wettability-altering effect of the CO₂-surfactant solutions were then evaluated (Figure 5B). For each surfactant, an oil-aged Eagle Ford shale chip was placed in the pressure cell, along with surfactant (10 mg) and a magnetic stir bar. The cell was sealed and heated to 80 °C. CO₂ (10 g) was added slowly to the cell and pressurized to 27.6 MPa using an ISCO pump. After the pressure stabilized, the magnetic stirrer was turned on and the oil-aged Eagle Ford shale chip was allowed to soak in the CO₂+surfactant solution for 16 h. When the soaking period was complete, the magnetic stirrer was turned off and pure CO₂ (50 mL) was pumped into the cell to displace the CO₂+surfactant solution. The cell was slowly depressurized and cooled. The sample was removed from the cell and the contact angle of a water droplet on the shale chip in air was measured at ambient pressure and temperature. This process was repeated for each of the three surfactants in this study.

2.5. CO₂-Oil IFT measurements. IFT measurements were performed using the pendant drop method using a Krűss DSA 10 apparatus equipped with a customized 30-mL view cell rated to 150 °C and 103 MPa.61 In the measurement with no surfactant present, CO2 (10 g) was first added to the cell and pressurized to 27.6 MPa using an ISCO pump. The cell was heated to 80 °C, then oil (3 mL) was added using a second ISCO pump. The CO₂ and oil phases were allowed to equilibrate overnight at 27.6 MPa. Next, oil was drawn from the bottom of the cell and used to generate a 2.5-µL pendant oil droplet through a 0.16 cm needle at the top of the cell. Temperature and pressure were kept constant throughout the experiment. The shape of the oil droplet was analyzed using Krűss Advance software to determine the CO2-oil IFT. Measurements were repeated at least three times and the average IFT values are reported.

The process was repeated with SURFONIC* TDA-9 dissolved in the CO_2 phase (surfactants N-100 and L12-6 were not tested.) TDA-9 (10 mg) and a stir bar were placed in the cell. The cell was sealed, and CO_2 (10 g) was added to the cell and pressurized to 27.6 MPa using an ISCO pump. The magnetic stirrer was turned on for 1 h. Stirring was stopped, and oil (3 mL) was added to the bottom of the cell at constant pressure using a second ISCO pump. The pressure of the system was allowed to equilibrate overnight, with CO_2 , surfactant, and oil held at 80 °C and 27.6 MPa. Then, oil was withdrawn from the bottom of the cell and used to generate a 2.5- μ L pendant oil droplet through the needle from the top of the cell.

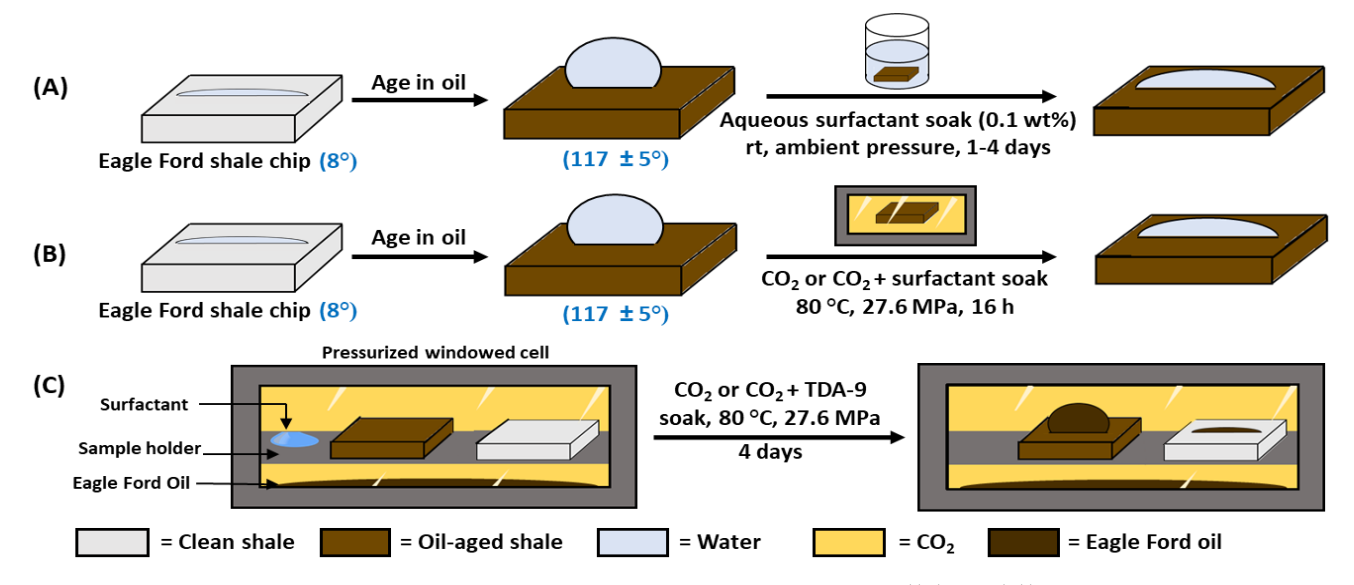


Figure 5. Workflow for ambient-pressure air-water-shale contact angle experiments ((A) and (B)), and high-pressure CO₂-oil-rock contact angle experiments (C). Air-water-shale contact angles are shown in parentheses.

2.6 CO₂-oil foaming experiments. A mixture of 65 wt% CO₂+0.1 wt% TDA-9 and 35 wt% Eagle Ford oil was observed at reservoir temperature (80 °C) and pressures (20.7, 27.6, 34.5, and 41.4 MPa) to determine whether the surfactant generates a CO₂-oil foam (SURFONIC® N-100 and L12-6 were not tested). These proportions and conditions were selected because they yielded approximately equal volumes of the CO₂-rich and oilrich phases in the CO2-oil mixture phase behavior experiments. The experiment was performed in the same windowed pressure cell as shown in Figure 4. SURFONIC® TDA-9 (37 mg) and Eagle Ford oil (20 g) were added to the Pyrex sample tube above the piston at rt. The sample tube was inserted into the phase behavior cell and the lid closed. The transparent overburden fluid, PDMS, was pumped into the bottom of the phase behavior cell to compress the oil and surfactant to 13.8 MPa. Liquid CO₂ (37 g) was pumped into the cell and the valve at the top of the cell was closed. The cell was then heated to 80 °C by a circulating air bath. The mixture was compressed to 20.7 MPa and stirred (2,000 rpm) for 10 min. Mixing was stopped and the mixture was immediately observed to determine whether any foam was generated at the interface between the CO₂-rich and oil-rich phases. The pressure was increased in increments of 6.9 MPa up to 41.4 MPa. At each pressure, the mixture was stirred for 10 min and then observed to determine whether a foam was generated.

2.7. High-pressure shale-oil-CO2 contact angle meas**urements.** The behavior of oil droplets on shale in CO₂ was observed at high pressure and temperature (27.6 MPa, 80 °C). Shale chips were not soaked in water prior to high-pressure contact angle measurements for consistency with other experiments in this study, and because adding water as an additional fluid phase may have complicated the measurement. Two outcrop Eagle Ford shale chips were cleaned for 5 min using a Harrick Plasma Cleaner. One of the shale chips was aged in Eagle Ford oil for two weeks and one was not aged. The two chips were placed on the sample holder in a customized windowed Hastelloy high-pressure, high-temperature cell, which has been described in a previous publication (Figure 5C). 62 Eagle Ford oil (3 ml) was added to the bottom of the cell, below the sample holder The cell was pressurized with CO₂ (41 g) to 6.9 MPa, and then the cell was heated to 80 °C.

Once the temperature was stabilized, the pressure was raised to 27.6 MPa using an ISCO pump. The $\rm CO_2$ and the oil in the bottom of the cell were allowed to equilibrate. In a separate pressure vessel, Eagle Ford oil (5 g) was equilibrated with $\rm CO_2$ (1 g) at 80 °C and 27.6 MPa. Droplets of $\rm CO_2$ -equilibrated oil were placed on the shale surface using a 0.16 cm needle after one day and, at another point on the sample, after four days. The droplets were observed using a Leica NC 170HD camera with a Z16 APO zoom system along with a Telocentric HP blue illuminator.

This process was repeated with TDA-9 (0.1 wt%) dissolved in the CO_2 . SURFONIC* TDA-9 (37 mg) and a stir bar were placed on the sample holder, away from the shale chips to avoid any mixing of surfactant and crude oil. CO_2 (37 g) was added up to 6.9 MPa, the temperature increased to 80 °C, and the system was pressurized to 27.6 MPa. The mixture was stirred for 1 h, then stirring was stopped and the system allowed to equilibrate overnight. Droplets were formed with CO_2 -equilibrated oil after one day and, at other points on the samples, after four days.

2.8. Huff-n-puff experiments. Cores were cut to the desired size (5.1 cm length \times 2.5 cm diameter) and their absolute permeabilities and porosities were measured using a TEMCO Helium Porosimeter HP-401 (Table 2). A new core was used for each huff-n-puff experiment. After being weighed, cores were placed in a high-pressure vessel and vacuumed (-65 KPa) for 48 h. Cores were then saturated with oil by isolating the vacuum pump and slowly adding Eagle Ford crude oil to the vessel. The cores were aged in crude oil at 50 °C and 27.6 MPa for at least eight days. The first time this aging process was performed, the shale core was removed from the oil every other day and weighed. After eight days, no further changes in core weight were observed. Thus, we determined that eight days was the optimal aging period for shale cores. Once saturated, the cores were removed from the pressure vessel, wiped to remove any surface oil, and weighed to determine the initial oil-in-place.

For unconfined huff-n-puff measurements, an oil-aged Eagle Ford or Mancos core was placed in a pressure cell (5.7 cm length \times 3.2 cm inside diameter) housed within an oven (Figure 6A). The empty volume around the core was designed

to allow the core to be fully immersed in CO₂ or CO₂+surfactant solution during the soaking period. In huff-n-puff experiments involving CO₂+surfactant solutions, the surfactant (20 mg or 2 mg) and a stir bar were added to the smaller section of the cell and the oil-aged shale core was placed in the larger section of the cell. The cell was sealed and heated (80 °C). The temperature was allowed to equilibrate for 45 min. CO₂ (20 g) was added slowly and pressurized to 27.6 MPa using an ISCO pump. After the pressure of the system equilibrated, the magnetic stirrer was turned on for a soaking period of 20 h. The cell was then slowly depressurized, the CO2 was vented, and oil was collected in a 20-mL vial. The core was removed from the cell, any oil on the core surface was wiped off, and the core was weighed to determine the amount of oil extracted. The core was kept at rt for 3-4 h until the weight of the core stabilized. Then, the core, stir bar and surfactant were added to the cell again and the process repeated for five cycles.

Confined huff-n-puff experiments were performed in a similar manner as described above. Bakken cores were aged in oil, confined in a Viton TM sleeve and placed in the pressure cell (Figure 6B). After CO_2 or CO_2 +surfactant soaking, the core was removed from the pressure cell and the sleeve was removed. The core was kept at rt for 3-4 h until the weight of the core stabilized. Some oil was produced from the sides of the core after the sleeve was removed. This oil was wiped from the

sides, and the core was weighed to determine the amount of oil extracted. The core was re-confined in the VitonTM sleeve for the next cycle.

2.9. Gas Chromatography. Oil produced during confined huff-n-puff experiments was analyzed by GC-MS. GC-MS data was not collected for oil extracted during unconfined huff-n-puff experiments. Sample preparation and GC-MS analysis methods were adapted from Hawthorne et. al.⁶³ After each cycle, the huff-n-puff chamber was depressurized, and the CO2 stream was collected into a 20-mL vial. The CO2 dissipated, leaving oil in the vial. The oil was diluted with dichloromethane (DCM) to a volume of 10 mL, and 1 mL of this oil in DCM solution was transferred to a GC vial. A solution of internal standard (octadecylbenzene, 99.5% purity, 0.2 mg/mL in DCM) was prepared, and 0.5 mL of the internal standard solution was added to the GC vials. Samples were analyzed using an Agilent 6890 gas chromatograph equipped with an Agilent 5975 mass spectrometer. A Perkin Elmer Elite 5-MS column (30 m long, 0.25 mm internal diameter, 0.25 μm film thickness) was employed. Samples were injected using an Agilent 7683 series injector (2 µL, injection port temperature 350 °C, splitless injection). The GC oven temperature was 30 °C with a 4 min hold, ramped 30-350 °C at 8 degrees/min, followed by a 20 min hold at 350 °C. The MS transfer line temperature was 300 °C.

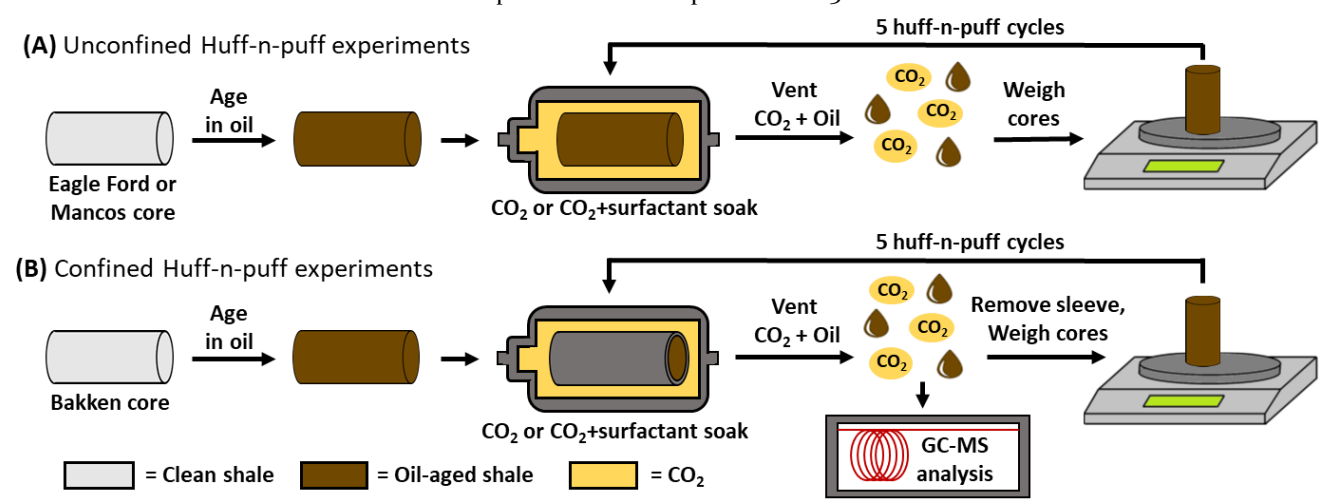


Figure 6. Workflow for (A) unconfined huff-n-puff experiments and (B) confined huff-n-puff experiments.

Table 2. Fluids and cores used in CO₂ and CO₂+surfactant huff-n-puff experiments.

= Unconfined = Confined

Core	Fluid ^a	Formation	Length (cm)	Diameter (cm)	Permeability (μD)	Porosity (%)	Dry Weight (g)	Oil-Aged Weight (g)				
1	CO ₂	Eagle Ford	5.02	2.55	<15	6.55	56.11	58.24				
2	CO ₂ + TDA-9 (0.10 wt%)	Eagle Ford	4.52	2.56	<15	7.78	50.32	52.29				
3	CO ₂ + TDA-9 (0.01 wt%)	Eagle Ford	4.72	2.56	<15	7.48	52.49	54.56				
4	CO ₂ + N-100 (0.10 wt%)	Eagle Ford	5.03	2.55	<15	7.22	55.99	58.24				
5	CO ₂	Mancos	4.38	2.53	7.27	5.13	55.14	56.01				
6	CO ₂ + L12-6 (0.10 wt%)	Mancos	5.10	2.54	76.20	4.61	64.51	65.55				
7	CO ₂ + L12-6 (0.01 wt%)	Mancos	5.04	2.53	9.31	3.50	63.50	64.66				
8^b	CO ₂	Bakken	5.26	2.50	9.86	6.20	64.52	65.94				
9^b	CO ₂ + TDA-9 (0.01 wt%)	Bakken	5.06	2.50	28.36	6.34	61.96	63.52				

^a Surfactants were obtained from Indorama SURFONIC^{*}. ^b Cores were confined with a Viton[™] sleeve during the CO₂ soak period.

3.1 CO₂-oil pressure-composition (Px). The Px diagram for CO₂-Eagle Ford oil mixtures ranging from 0-100% CO₂ is shown in Figure 7. The curve at lower CO₂ composition (o-38 wt%), labelled "100%", represents the bubble point curve, and the curve at higher CO₂ compositions (38-70 wt%), labelled "0%" represents the cloud point curve. 64 The blue region above the bubble point and cloud point curves represents the single phase region, wherein CO₂ and oil are miscible. Below the bubble point and cloud point curves, the mixture exists in two phases—an oil-rich liquid phase and a CO₂-rich fluid phase. At higher pressures, the CO₂ phase had a liquid-like density, and at lower pressures, the CO₂ phase had a gas-like density. Throughout the twophase region, the relative volumetric proportions of CO₂rich and oil-rich phases were determined. The values next to each data point indicate the vol% of oil-rich liquid phase relative to the total two-phase mixture. The values in the boxes correspond to the curves of constant vol% of the oilrich liquid phase in the mixture.

The Px diagram indicates that CO2 and oil are immiscible at higher compositions of CO₂, even at high pressures. For example, at 25 MPa, CO2 and oil form two immiscible phases at compositions above 40 wt% CO2. At very high pressure of 62 MPa (the operational pressure limit of our cell), CO₂ and oil are still immiscible at compositions above approximately 70 wt% CO₂. Therefore, 70 wt% CO₂ represents the miscibility gap—the composition above which components are immiscible, regardless of pressure (here, up to 62 MPa). A similar miscibility gap has been previously reported in other CO2-oil phase behavior studies. 65, 66 Therefore, even though CO₂ is considered a good solvent for oil, there are still a wide range of conditions in which the two fluids are immiscible. The presence of a CO2-oil interface (or CO₂-oil-shale interface) indicates that a surfactant could improve oil extraction either by wettability alteration or IFT reduction.

In experiments related to CO₂ EOR in conventional reservoirs, where CO2 flows through porous rock to extract oil, the miscibility between CO₂ and oil is traditionally measured using the slim tube test, wherein CO2 is injected into a sand-packed slim tube saturated with oil. By the slim tube method, the minimum miscibility pressure (MMP) of the of the CO₂-Eagle Ford system is only 14.7 MPa at 77 °C.49 However, the Px data shown in Figure 7 indicates that there exists a range of conditions, especially at higher CO₂composition, where Eagle Ford oil and CO₂ are immiscible, even at pressures far above the MMP. The low MMP value obtained by the slim tube test is due to the ability of CO₂ to increase miscibility with oil as it moves through a porous matrix collecting hydrocarbons—a process referred to as multiple contact miscibility (MCM). In unconventional reservoirs, where CO₂ is injected through fractures and allowed to soak into the rock over time, oil is primarily extracted by diffusion and MCM does not occur. Therefore, the conclusion that CO₂ and oil are miscible in unconventional reservoirs at pressures above the traditional MMP would be inaccurate. Rather, as the phase behavior diagram indicates, CO2 and oil are immiscible at high CO2 compositions and thus, a surfactant can improve CO₂ EOR.

The Px diagram presented in this study was generated using mixtures of CO2 and a dead Eagle Ford crude oil at 80 °C. Although we did not have the resources to generate an analogous Px diagram for a live Eagle Ford crude oil, it is possible to estimate the effect of adding volatile components (e.g. C1-C4) to the crude oil. The bubble point pressure of dead oil alone (i.e. 100% dead oil, 0% CO2) is approximately o MPa. Therefore, the bubble point curve shown in Figure 7 approaches a value of o MPa on the left side of the Px diagram where the mass fraction of CO₂ is o%. However, if the volatile components of a live oil were included, then the live oil bubble point curve would shift upwards such that the Y-intercept would be equal to the bubble point pressure of live Eagle Ford crude oil (12.9 MPa, 80 °C)⁶⁷ at o wt% CO₂. The entire bubble point curve would be expected to shift upwards by a comparable amount. Relative to mixtures of CO2 and dead oil, higher pressures are required to compress mixtures of CO2 and live oil into a single phase. Therefore, the critical point and cloud point pressure curve would also shift upwards. As a result, the two-phase liquid-fluid region would persist and become slightly wider at a given pressure.

3.2. Surfactant solubility measurements. Px diagrams for the three different surfactants in CO₂ were obtained at 25 °C, 58 °C, 77 °C, and 100 °C (Figure 8).68 A single-phase region occurs above each curve, where the surfactant is fully soluble in CO2. A surfactant-rich liquid phase begins to precipitate out of solution at the pressure corresponding to the cloud point curve. Below the curve, the mixture exists in two phases. The cloud point pressure increases with increasing temperature for a given composition and increases with increasing concentration at a given temperature. The huff-n-puff operating conditions of this study (27.6 MPa and 80 °C) are above the cloud point pressures for a given mixture of surfactant (0.1 wt%) and CO₂ (approximately 20 MPa), which ensures that the surfactant is completely dissolved in CO2 during huff-n-puff experiments (Figure 8A).

The cloud point pressures in this study are lower than those previously reported for SURFONIC* TDA-9 and N-100 at 25 °C and 58 °C.^{27, 28, 69} This difference is likely due to lower concentration of CO₂-insoluble impurities present in the surfactants used in the current study. Previously, during the proprietary synthesis of these nonionic surfactants, a small amount of CO₂-insoluble, surfactant-soluble salt was formed and remained within the product. This impurity was the first compound to come out of solution during the expansion of the CO₂-surfactant mixture, increasing the apparent cloud point of the mixture. The current synthetic technique for making the surfactants is more likely to have a lower concentration of this CO₂-insoluble salt, leading to a lower cloud point pressure than previously reported.

At ambient pressure, each of these surfactants is completely miscible with water and Eagle Ford brine⁶⁰ at rt and 77 °C. They are less than 1.0 wt% soluble in Eagle Ford crude oil at rt, and approximately 1.0 wt% soluble in Eagle Ford crude oil at 77 °C.

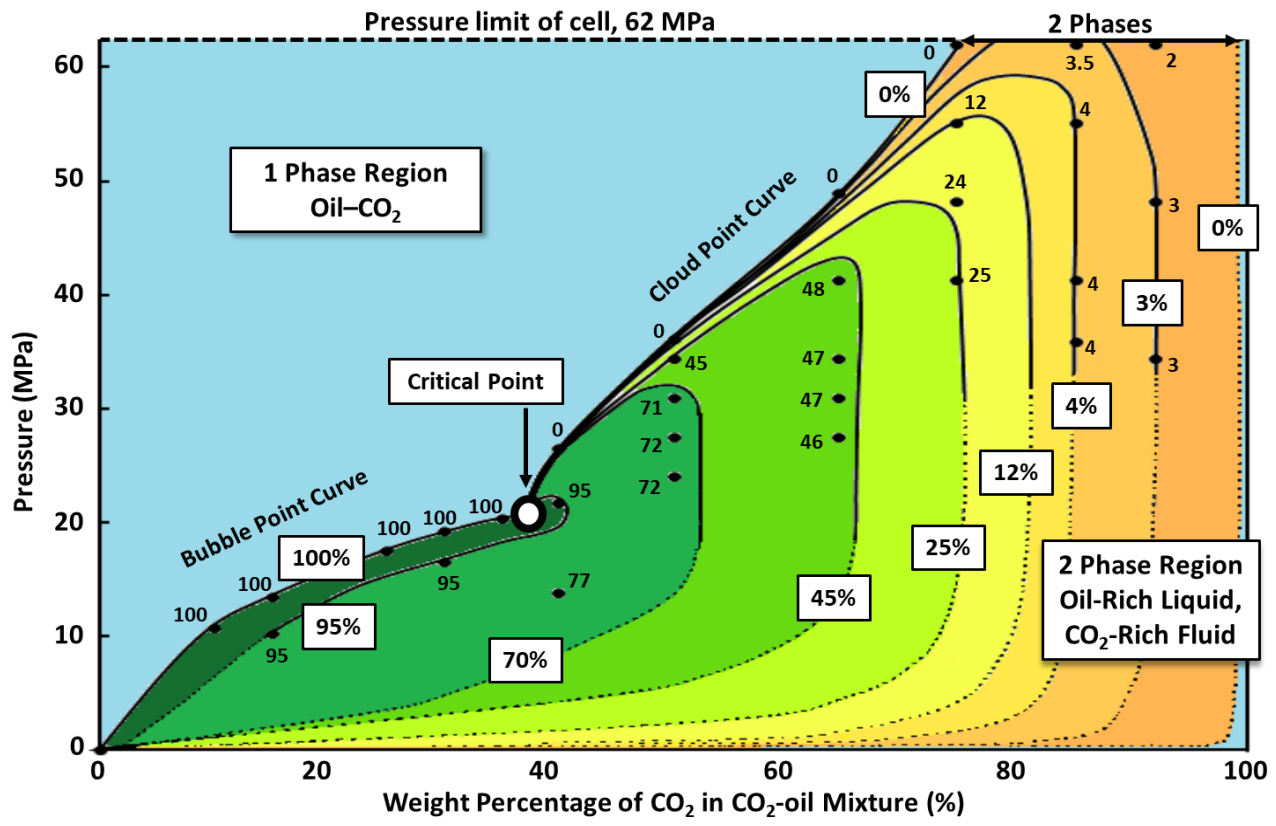
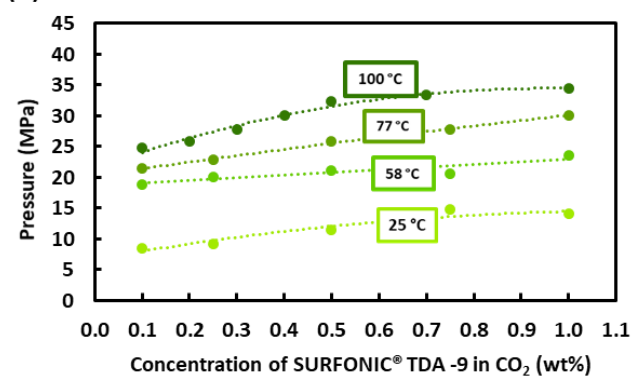
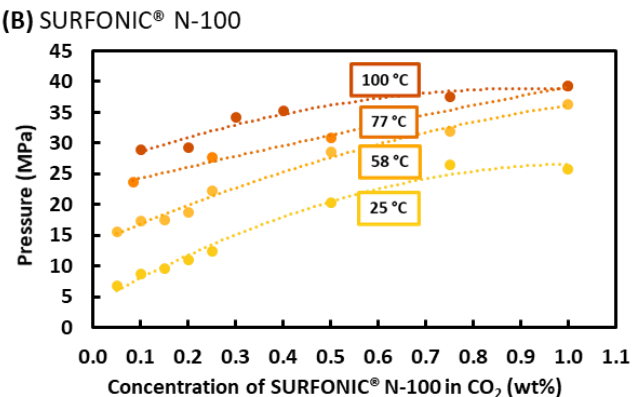


Figure 7. Pressure-composition diagram of the pseudo-binary mixture of CO_2 and Eagle Ford crude oil at 80 °C. The values in the boxes correspond to the curves of constant vol% of the oil-rich liquid phase relative to the total mixture. Note that the actual position of the nearly vertical cloud point boundary of the two-phase region (at the right-hand side of the figure, close to the 100% CO_2 value) was not determined. At pressures above approximately 55 MPa in the two-phase region, a phase inversion occurred, as the CO_2 -rich phase became the denser phase.







(C) SURFONIC® L12-6

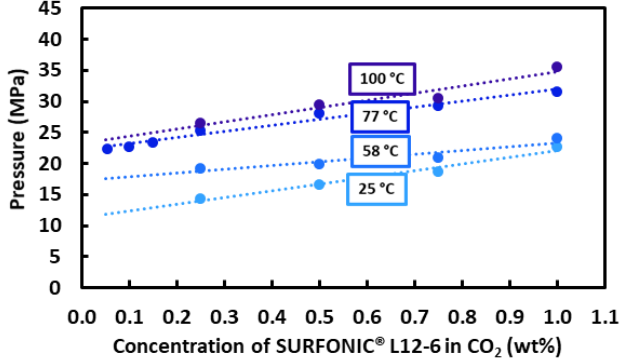


Figure 8. Px diagrams exhibiting cloud point curves for the surfactant-CO₂ mixtures. The five cloud point pressures values for each mixture at a specified temperature were were within 0.5 MPa of the illustrated average data; which is consistent with the size of the data markers.

3.3. Ambient pressure shale-water-air contact angle measurements. In this section, "water-wet" corresponds to contact angles of o-70°, intermediate-wet corresponds to contact angles of 70-110°, and "oil-wet" corresponds to contact angles greater than 110°.7°

After cleaning, the Eagle Ford shale chips were strongly water-wet. A water droplet immediately flattened once it touched the surface of the rock, giving a contact angle of 8°. After aging chips in Eagle Ford crude oil for two weeks at 80 °C, a water droplet made a contact angle of 117±5° with the rock surface at rt, indicating that the aging process successfully rendered the outcrop shale chips oil-wet (Figure 9A). After soaking the oil-wet shale chips in aqueous solutions containing 0.1 wt% of surfactants, the contact angles

of water droplets on the shale chips in air changed from 117±5° to 66° for SURFONIC* TDA-9, 28° for SURFONIC* N-100, and 41° for SURFONIC* L12-6 (Figure 9B). SURFONIC* TDA-9 effected a dramatic change in contact angle after soaking only 24 h. In soaking experiments involving the other two surfactants (N-100 and L12-6), longer soaking times were required to achieve maximum wettability changes (2 days and 4 days, respectively). These results demonstrate the ability of the surfactants to alter the oilwet surface of the shale toward water-wet.

An oil-aged Eagle Ford shale chip was soaked in CO₂ without surfactant at 27.6 MPa and 80 °C for 16 h. The contact angle of a water droplet on the shale surface was then measured. No discernible effect on the shale wettability was observed. The contact angle was 118°, nearly identical to 117°, the original contact angle of the aged Eagle Ford sample (Figure 9C). This result indicates that under these conditions, CO₂ alone did not alter the wettability of the oil-wet Eagle Ford shale. Because the conditions of this experiment (80 °C, 27.6 MPa, high vol% CO₂) corresponded to the two-phase region of the Px diagram (Figure 6), the CO₂ may not have removed oil from the shale surface because the two phases were immiscible. If even a thin film of oil or oil-wetting deposits was left on the shale, the wettability could remain unchanged.

Alharthy et al. previously reported that pure CO₂ induced a shift in wettability from oil-wet to water-wet.71 In that experiment, an oil-aged shale chip from the Three Forks formation was soaked in CO₂ for two days at 17.2 MPa—a pressure commensurate with the CO₂-Bakken oil MMP at 100 °C. The contact angle photographs were taken at ambient temperature and pressure. Because the oil droplets float up to a shale surface, we assume that the continuous phase is water rather than air. The difference in our results could be due to the longer soaking time of that experiment or the different continuous phase employed in their measurements. Furthermore, the use of two different crude oils in each experiment could cause different results. CO₂ and Bakken oil may be more miscible at the experimental pressure and temperature (17.2 MPa, 100 °C) than Eagle Ford oil is at the conditions employed in our study (27.6 MPa, 80 °C,).

Oil-aged Eagle Ford shale chips were soaked in CO2 containing 0.1 wt% surfactants at 80 °C and 27.6 MPa for 16 h. The three surfactants tested are all soluble in CO₂ at these conditions (Figure 8). After soaking, the contact angle of a water droplet on shale in air was reduced to 67° for SURFONIC® TDA-9, 44° for SURFONIC® N-100, and 39° for SURFONIC[®] L₁₂-6[®] (Figure 9D). In the cases of TDA-9 and L12-6, the contact angles of the CO₂ and aqueous surfactant soaks were nearly identical. In contrast, the contact angle after soaking in CO₂-N-100 solution (44°) was higher than the contact angle after soaking in aqueous N-100 solution (28°). We do not have an explanation for this observation based upon the surfactant chemistry, but attribute this difference to experimental variability. Overall, these results demonstrate that a dilute concentration of surfactant enhanced the ability of CO2 to shift the wettability of the shale sample away from oil-wet and toward water-wet. Either the surfactant deposited on the shale to alter

wettability, or the CO₂-surfactant solution had an enhanced ability to clean oil-wetting *deposits* from the shale surface by micellar solubilization.

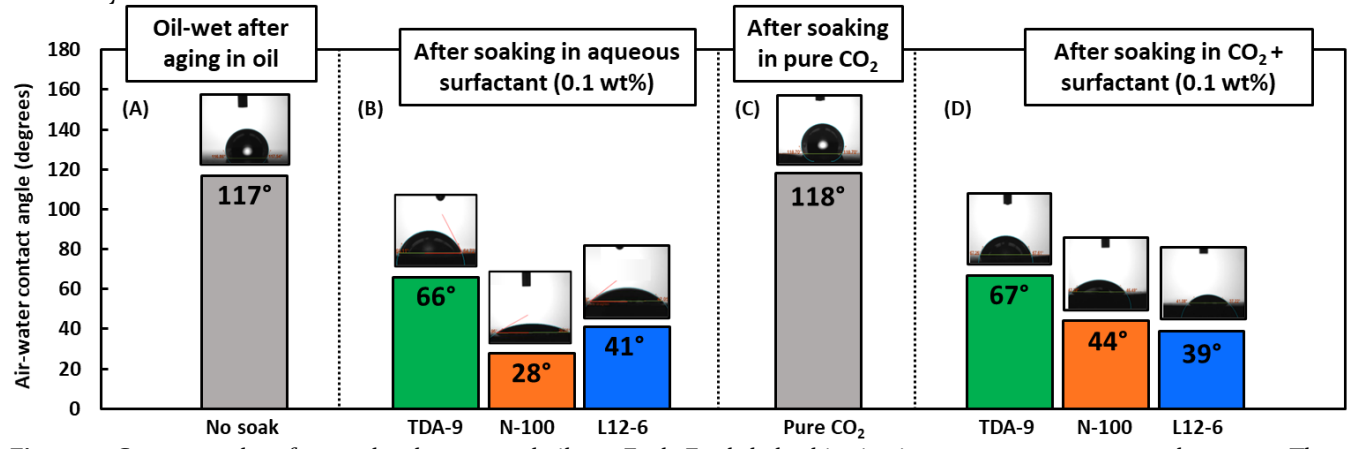


Figure 9. Contact angles of water droplets on aged oil-wet Eagle Ford shale chips in air at room temperature and pressure. Three measurements were taken on each shale chip, at different points on the sample. At each condition, all contact angle values were within 2° of the average value indicated in the figure. (A) Oil-wet Eagle Ford shale chip after aging in oil for two weeks. (B) Shale chips shift to water-wet after soaking in aqueous surfactant solutions for 1 day (TDA-9), 2 days (N-100) and 4 days (L12-6). (C) No change in contact angle after soaking in high-pressure CO₂ (27.6 MPa, 80 °C) for 16 h. (D) Shale chips shift to water-wet after soaking in high-pressure CO₂+surfactant solutions (27.6 MPa, 80 °C) for 16 h.

3.4. CO₂-Oil IFT measurements. The effect of one surfactant, SURFONIC® TDA-9, on CO₂-oil IFT was evaluated. The IFT between pure CO2 and Eagle Ford oil was 0.55 mN/m at 27.6 MPa and 80 °C (Figure 10A). This value is lower than the values for CO₂-oil IFT values reported in the literature (2-4 mN/m), which were measured at lower pressures.34, 35, 36, 37 In our IFT measurement, CO2 (10 g) and oil (3 ml, 2.3 g) were equilibrated prior to the IFT measurements. Based upon the Px diagram, this mixture (81 wt% CO₂, 19 wt% oil) at 80 °C and 27.6 MPa is in the two-phase region with the oil-rich liquid phase and CO2-rich fluid phase, comprising approximately 12 vol% and 88 vol% of the mixture, respectively. Because this is a pseudo-binary diagram (the oil is a multicomponent mixture), the precise equilibrium phase compositions cannot be obtained from this diagram. However, the mixture is in the two-phase region at a pressure (27.6 MPa) greater than the critical pressure (20 MPa) and greater than the MMP reported in the literature (14.7 MPa, 77 °C).49 Thus, the Px diagram indicates that a substantial amount of CO2 is dissolving in the oil-rich phase and a portion of the oil components are dissolving in the CO₂-rich phase. Therefore, the low IFT between these two equilibrium phases is not surprising.

The presence of the CO₂-soluble surfactant, SURFO-NIC* TDA-9 in the CO₂ phase did not lead to a reduction of IFT. The IFT remained approximately the same, at 0.61 mN/m (Figure 10B). Because the IFT between CO₂ and oil at this high pressure and temperature is already low, a large reduction in IFT upon addition of surfactant was not expected. Further, the chemical structure of TDA-9 makes IFT reduction unlikely. Because both the alkyl and PEO groups on TDA-9 have some degree of CO₂-philicity, the surfactant does not reduce IFT as well as a surfactant with CO₂-philic groups would be expected to. In lower-pressure environments, surfactants with more CO₂-philic groups, such as oil-soluble alkyl-silicone surfactants,³⁹ and CO₂-

soluble alkyl propoxylated surfactants, have been shown to decrease $\rm CO_2\text{-}oil\ IFT.^{56}$

Based upon our current results for the inexpensive ethoxylated alcohol surfactants used in this study, we do not expect that IFT reduction is the mechanism by which CO₂ EOR is improved using surfactants. Fortunately, when surfactants are intended to enhance oil recovery in low-permeability reservoirs, a large change in wettability from oilwet to water-wet with little or no change in IFT is desired.^{3, 24}

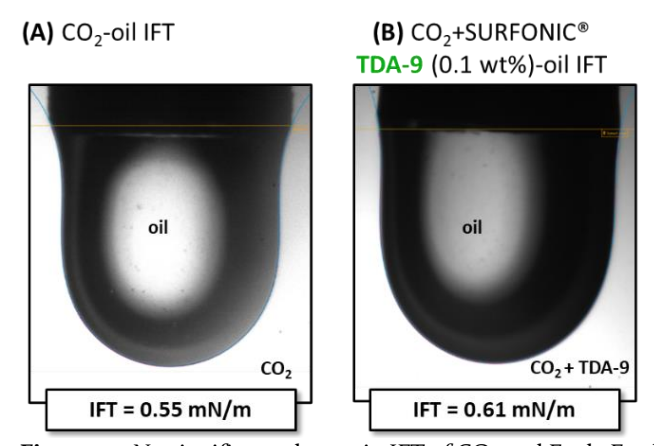


Figure 10. No significant change in IFT of CO_2 and Eagle Ford oil after addition of SURFONIC TDA-9 (0.1 wt%) to CO_2 at 80 °C and 27.6 MPa.

3.5 CO₂-oil foaming experiments. The ability of one surfactant, SURFONIC* TDA-9, to generate CO₂-oil foams at reservoir temperature and pressures (80 °C, 20.7, 27.6, 34.5, and 41.4 MPa) was tested. The CO₂-oil composition used in this experiment (65 wt% CO₂, 35% Eagle Ford oil) was selected because it affords two approximately equal-volume phases—an oil-rich liquid phase and a CO₂-rich

fluid phase—at the range of pressures tested (Figure 7). The range of pressures was selected to ensure that the surfactant was soluble in CO_2 at 80 °C (minimum pressure, 20.7 MPa) and that the CO_2 -oil mixture remained in the two-phase region (maximum pressure, 41.4 MPa).

After mixing CO₂ and oil in the presence of TDA-9, no foam was observed at any pressure from 20.7 to 41.4 MPa—either in the form of bubbles of CO₂ within films of oil, or bubbles of oil separated by films of CO₂. Therefore, at these conditions, TDA-9 is not expected to generate a CO₂-oil foam when injected into an unconventional reservoir. These results are consistent with our prior studies, in which it was shown that CO₂-in-oil foams are extremely difficult to generate with oil-soluble or CO₂-soluble surfactants.^{38, 72, 73} Here, the absence of foam generation by the addition of TDA-9 to the CO₂-oil mixture, in combination with IFT and contact angle experiments, indicates that the expected mechanism of increased oil recovery by CO₂-dissolved nonionic surfactants is wettability alteration, rather than conformance control or CO₂-oil IFT reduction.

3.6. High-pressure shale-oil-CO₂ contact angle measurements. High-pressure contact angle experiments were conducted in which droplets of Eagle Ford oil were placed on Eagle Ford shale chips at 80 °C and 27.6 MPa in the presence of CO₂ or CO₂-surfactant solutions (Figure 11). This experiment directly tested the central hypothesis of this work—that CO₂-dissolved surfactants can alter the wettability of shale from oil-philic toward CO₂-philic. (Nonetheless, we also conducted the series of ambient pressure air-water-rock contact angle experiments, because of their simplicity and their ability to qualitatively indicate whether nonionic surfactants can alter wettability (Figure 9).)

This high-pressure experiment was challenging for two reasons. First, controlling the size of the droplet—which is always a challenge in contact angle measurements—was even more difficult here because of the need to completely vent the system if droplets were unsuitable for measurements. A second challenge was the difficulty of equilibrating the CO2 and oil phases prior to the contact angle measurements. Although CO2 and oil form two phases at the experimental temperature and pressure, lighter components of oil are still extracted by CO₂ and some CO₂ is dissolved in the oil. Therefore, in order to establish distinct interfaces, the CO₂ and oil must be equilibrated first. The fluids in the mixing vessel and the measurement vessel were equilibrated prior to the experiments, However, the oil in the needle and the tubing could not be completely equilibrated. While one of our results yielded a clear image of the CO₂, oil and rock (Figure 11B), the other CO₂-oil-rock interfaces were not as distinct. For example, the ripples coming out of the needle in Figures 11 A, C, and D are caused by light hydrocarbons being extracted by CO₂. Because of the imperfection of the droplets and the haziness of the CO₂-oil boundary in some images, the contact angle results shown in Figure 11 considered as reasonable but not highly precise estimates.

These high-pressure contact angle experiments were performed on two shale chips: one that was clean and one that was aged in Eagle Ford oil. In the absence of

surfactant, oil spread on both the oil-aged and clean shale chips (Figure 11, A and B, contact angles of 11° and 14°, respectively). This result indicates that the shale surface has an affinity for oil when submerged in CO2, regardless of whether the shale chip was aged in oil or not. After soaking in CO₂+0.1 wt% TDA-9 solution for four days, oil beaded up on the oil-aged shale chip and attained an intermediate wettability value of 82°, but spread on the clean shale chip with a much more modest shift (to a contact angle of 39°) (Figure 11, C and D). This observation supports the proposed mechanism of surfactant adsorption illustrated in Figure 1. The oil-aged shale chip has a layer of oil-wetting deposits and producible oil covering the mineral surface. The oil-philic hydrocarbon segment of the surfactant adsorbs to the oil layers, with the oil-phobic PEO segments aligned outward toward the CO₂. These results are, to the best of our knowledge, the first reports of a favorable, surfactant-induced altered wettability away from oil-wet toward intermediate CO₂-oil wet in a high-pressure CO₂-oilrock environment.

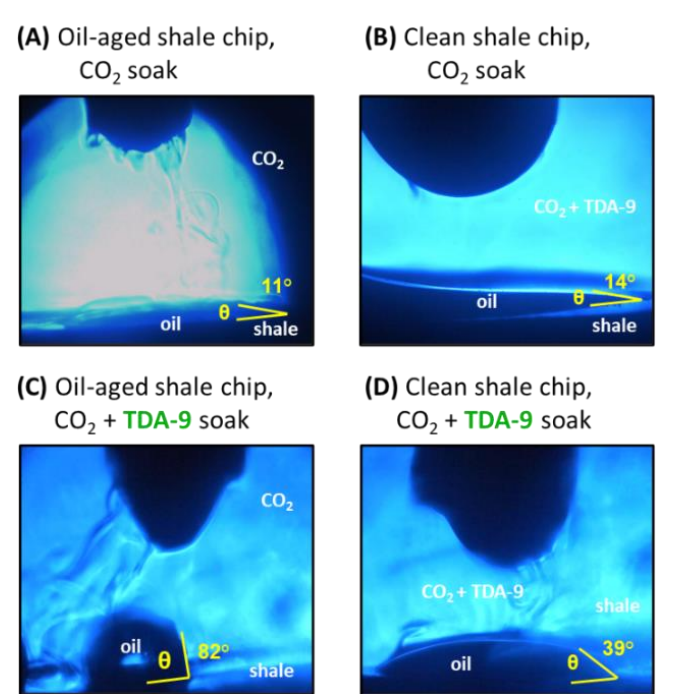


Figure 11. Droplets of Eagle Ford oil on shale chips in CO₂ at high pressure and temperature (27.6 MPa, 80 °C). Droplets spread on both oil-aged and clean shale chips in pure CO₂ ((A) and (B)). The distorted droplet shape on the bottom left side of (B) is due to interference from the sample holder. The oil droplet beaded up on an oil-aged shale chip in CO₂+SURFO-NIC* TDA-9 (0.1 wt%) (C). This change was less pronounced on a clean shale chip. Even with surfactant present, the oil droplet spread on a clean shale chip (D).

Figure 11 shows oil droplets that were placed on shale chips after the chips had been soaking for four days. Droplets were also placed on shale chips after soaking only one day (images not shown). After soaking for one day, droplets spread on all shale chips, including those soaking in CO_2 +0.1 wt% TDA-9 solution. This observation indicates that adsorption of the surfactant to the shale surface may

be time-dependent. Because this experimental set-up did not allow for continuous stirring of the surfactant in the CO₂, (stirring would have disrupted the oil droplets), complete dissolution of the surfactant was dependent on diffusion. Although the absence of a change in contact angle after only one day of soaking may have been caused by incomplete dissolution of the surfactant, it does indicate that longer soak times might enable better adsorption of the surfactant to the shale surface for optimal wettability alteration. In this case, significant wettability alteration by the surfactant was observed after four days.

3.7. Huff-n-puff experiments. Figure 12 shows the ultimate oil recovery (left) and incremental oil recovery after each huff-n-puff cycle (right) for Eagle Ford, Mancos, and Bakken cores. The effect of two surfactants, SURFONIC* TDA-9 and N-100, were tested using Eagle Ford cores (Figure 12A). After five cycles, the ultimate recovery reached 71% for pure CO₂ (black), 75% for CO₂+0.1 wt% SURFONIC* TDA-9 (green), 72% for CO₂+0.01 wt% SURFONIC* TDA-9 (light green), and 67% for CO₂+0.1 wt% SURFONIC* N-100 (orange). Huff-n-puff oil recovery increased with increasing concentrations of TDA-9 dissolved in CO₂. The most pronounced increases in oil recovery were observed in the first and second cycles. Throughout the remaining cycles, oil recoveries with CO₂+TDA-9 solutions were consistently higher than those of pure CO₂. During huff-n-puff

experiments with SURFONIC® N-100, however, oil recovery was lower than that of pure CO₂. The high incremental oil recovery of the fifth cycle of CO₂+0.1 wt% SURFONIC® N-100 was due to a long, three-day, weekend soak period. We are not certain why incorporation of N-100 decreased oil recovery compared to pure CO₂. This nonylphenol ethoxylate was the only surfactant that contained a rigid aryl group in its structure, which may have impacted its ability to diffuse into the core or to adsorb onto surfaces.

Unconfined huff-n-puff experiments using SURFONIC® L12-6 were performed using oil-aged Mancos cores (Figure 12B). After five cycles, the ultimate recovery reached 90% for pure CO2 (black), 84% for CO2+0.1 wt% SURFONIC® L12-6 (blue), and 91% for CO₂+0.01 wt% SURFONIC® L12-6 (light blue). In this set of experiments, the increasing amount of surfactant diminished oil recovery-even though the permeability of the core used for the experiment containing the highest amount of L12-6 (0.1 wt%) was an order of magnitude higher than those of the cores used for the pure CO₂ and the 0.01 wt% surfactant experiments (Table 2, entries 5-7). Again, we are not certain why this decrease in oil recovery occurred. This linear dodecyl ethoxylate contained the shortest PEO segment. Perhaps the PEO group was too short to impart the desired change in wettability to the shale surfaces.

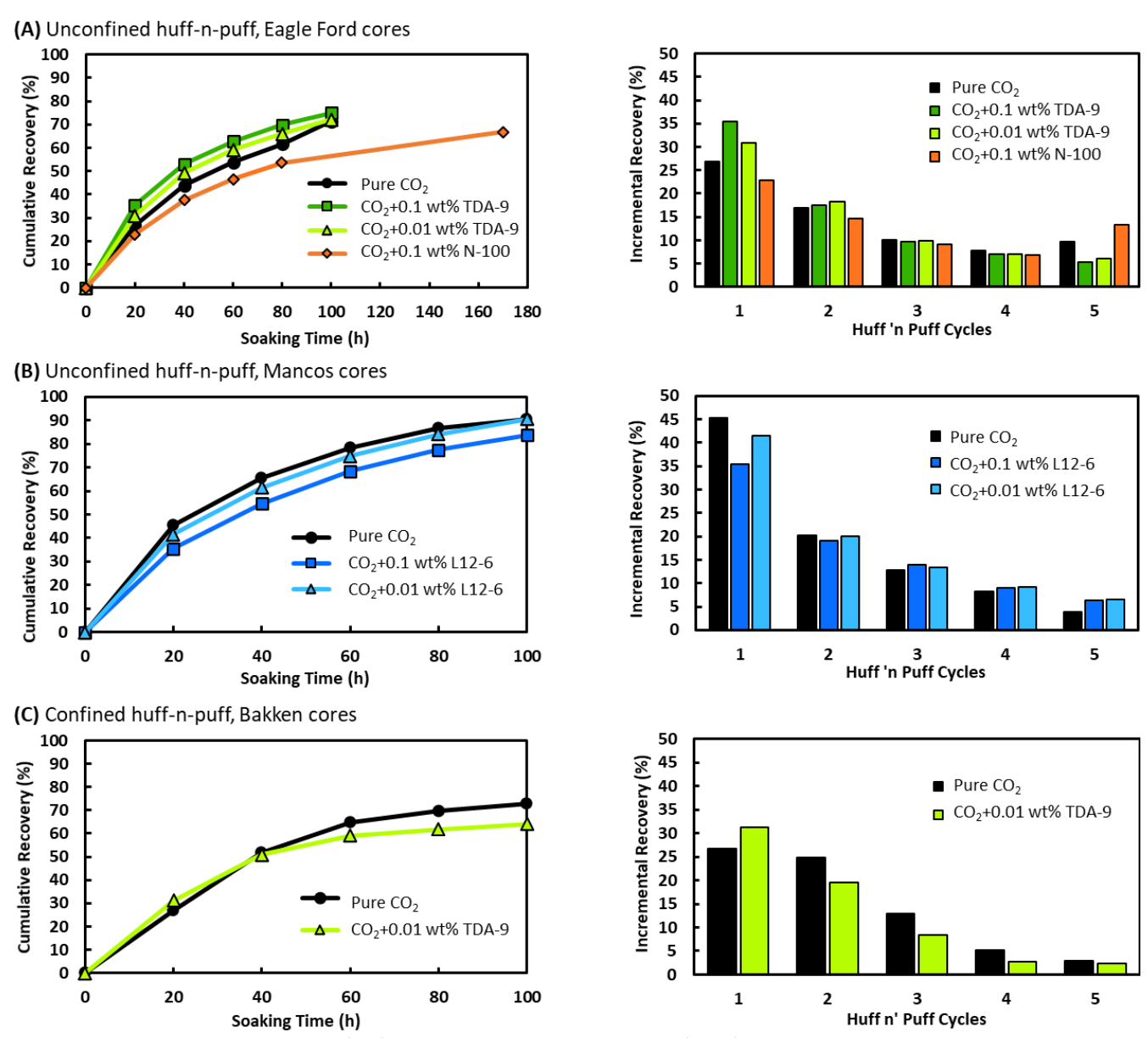


Figure 12. Ultimate oil recoveries (left) and incremental oil recoveries (right) obtained during huff-n-puff experiments using Eagle Ford (A), Mancos (B) and Bakken (C) cores.

Confined huff-n-puff experiments were performed using Bakken cores, wherein the core was confined using a VitonTM sleeve during the soak period so that only the ends were exposed (Figure 12C). Pure CO₂ afforded oil recovery of 73% (black), while CO₂+0.01 wt% TDA-9 recovered only 64% (light green). Although the surfactant solution afforded a lower ultimate oil recovery, the oil CO₂+0.01 wt% TDA-9 solution recovered more oil during the first cycle than pure CO₂, (31% and 27%, respectively). This ability of the surfactant to increase recovery in the first cycle was also observed in the unconfined huff-n-puff experiment using Eagle Ford cores (Figure 12A).

The ultimate oil recovery values for both confined huff-n-puff experiments were higher than expected, given that only the ends of the core were exposed to CO₂. This observation can be attributed to the fact that the VitonTM sleeves surrounding the cores had to be removed between cycles to weigh the cores. While the VitonTM sleeves were

removed, more oil was produced from the sides of the cores. The loss of this oil reduced the weights of the cores, resulting in higher oil recoveries being recorded.

It is difficult to draw conclusions about which surfactant performed best during huff-n-puff experiments because Eagle Ford cores were used in experiments involving SURFONIC® TDA-9 and N-100, Mancos cores were used in experiments involving SURFONIC® L12-6, and Bakken cores were used in confined huff-n-puff experiments. This difference was due to the availability of cores in our laboratory. The best performance was associated with the tridecyl ethoxylated alcohol with an average of nine EO groups; SURFONIC® TDA-9 (Figure 12A). More oil was recovered with increasing amounts of this surfactant in the unconfined Eagle Ford core. This increase was primarily attributable to a higher amount of oil recovered during the first cycle. Huff-n-puff experiments were not repeated and

thus, the experimental uncertainty of these results is unknown

3.8. Gas Chromatography. Produced oil collected during the confined huff-n-puff experiments using Bakken cores and SURFONIC® TDA-9 was analyzed by GC-MS (Figure 13). Lighter hydrocarbons (*n*-C6–*n*-C8) that were present in the Eagle Ford oil (Figure 3) but not observed after each huff-n-puff cycle were dissipated during CO2 venting. GC-MS analysis revealed differences in molecular weight distributions of the oil produced by CO₂ extraction, with and without a surfactant. Although the pure CO₂ without a surfactant produced more oil, the experiment with the surfactant preferentially produced heavier hydrocarbons, especially on the first cycle. This difference could be due to the ability of the surfactant to remove heavy hydrocarbons from the surface of the shale core by micellar solubilization. A similar observation was made by Zhang et al., in which an aqueous surfactant solution recovered darker, heavier oil fractions than water alone.⁴⁹ Averaged over all cycles, the CO2+0.01% TDA-9 solution employed in our study produced heavier oil compared to CO2 alone (average of 21.2 carbons, compared to 18.9 without a surfac-

3.9 Ability of CO2-dissolved surfactants to improve CO₂ EOR. This work probes, for the first time, whether surfactants dissolved directly in CO2 can add another mechanism—surfactant-induced wettability alteration to the long list of other mechanisms already known to promote oil recovery in unconventional formations during CO2 EOR. We confirmed that nonionic surfactants can dissolve in CO₂ at concentrations up to approximately 1 wt% at typical CO2 EOR conditions. We also confirmed that a miscibility gap exists for the CO₂-Eagle Ford crude oil mixture even at pressures much greater than the MMP, which indicates that there is an interface where a surface-active agent can favorably impact oil recovery. The nonionic ethoxylated surfactants were shown to have the ability to alter the wettability of an aged oil-wet shale in the desired direction from oil-wet toward water-wet (or CO₂-wet) at the laboratory-scale. The surfactant had no effect on the CO₂oil IFT, which was desired because lower IFT can reduce surfactant imbibition.3, 24 The surfactant also did not generate a CO2-oil foam. Wettability alterations were attributed to a surfactant adsorption to the oil-wetting deposits on the shale surface. Although nonionic surfactants exhibit lower shale adsorption than ionic surfactants (making them an economic choice in the field),74 we found that the adsorption was sufficient to enable wettability alteration. Unfortunately, we did not have the resources to assess nonionic surfactant adsorption quantitatively. In the best case (SURFONIC® TDA-9), the increase in oil recovery was on the order of one to four percentage points at dilute

concentrations of 0.01 and 0.1 wt%. The other two surfactants afforded lower oil recoveries than pure CO₂—indicating that there may be situations in which the introduction of a surfactant such as TDA-9 to CO₂ does improve oil recovery, but there are surfactants or rock/oil systems in which no benefit will be derived. Although the oil recovery increase by a surfactant dissolved in CO₂ was modest and the uncertainty in the data is not known, a several percentage point increase in oil recovery could be significant on the reservoir scale.

Oil recovery by CO₂-dissolved surfactants might be enhanced by improvements arising from future investigations of other types of CO2-soluble surfactants. For example, all surfactants in this study are relatively large, with lengths between 3.82-4.26 nm, about the size of n-C30 (Figure 14). Therefore, the surfactants may not be able to enter the small pores of the shale samples. Incorporation of smaller wettability-altering additives-such as 3-pentanone,75,76 or alkyl ethoxylates with fewer EO groups or shorter hydrocarbon segments—in the CO₂ phase could afford higher levels of oil production. For example, 3-pentanone is 0.61 nm long, about the length of n-C5 and would be more likely to penetrate the shale matrix to change wettability at the pore scale. Further, the study of nonionic propoxylated surfactants should be considered, as the poly(propylene oxide) (PPO) moiety is more CO₂-philic that the PEO moiety. However, the PPO group is also more oil-philic and less hydrophilic than PEO. Regardless of the alkyl group, the surfactant will be water-insoluble and therefore inappropriate for any water-based use. Therefore, propoxylated surfactants are not certain to outperform ethoxylated surfactants in this application, but there is merit in assessing that surfactant class.

Although more work is needed to optimize surfactant structures, the ability of CO2-dissolved nonionic surfactants to change the surface properties of shale has been demonstrated. One of the advantages of waterflooding as an EOR strategy in unconventional reservoirs is the ability of water to be modified through dissolution of salts, surfactants, and other chemical additives. Here, we show that CO2 can also be modified for EOR in shale through dissolution of surfactants. Thus, wettability alteration by surfactants can be combined with the other mechanisms by which CO₂ increases oil recovery. We anticipate that, as anthropogenic CO₂ becomes more available through CO₂capture efforts, that CO₂ EOR in unconventional reservoirs will provide an important economic driver for anthropogenic CO₂ capture and result in more CO₂ being stored permanently in the subsurface.⁷⁷ Improvement of the oil-extracting ability of CO2 through surfactants can increase its use as an EOR fluid, affording both environmental and economic benefits.

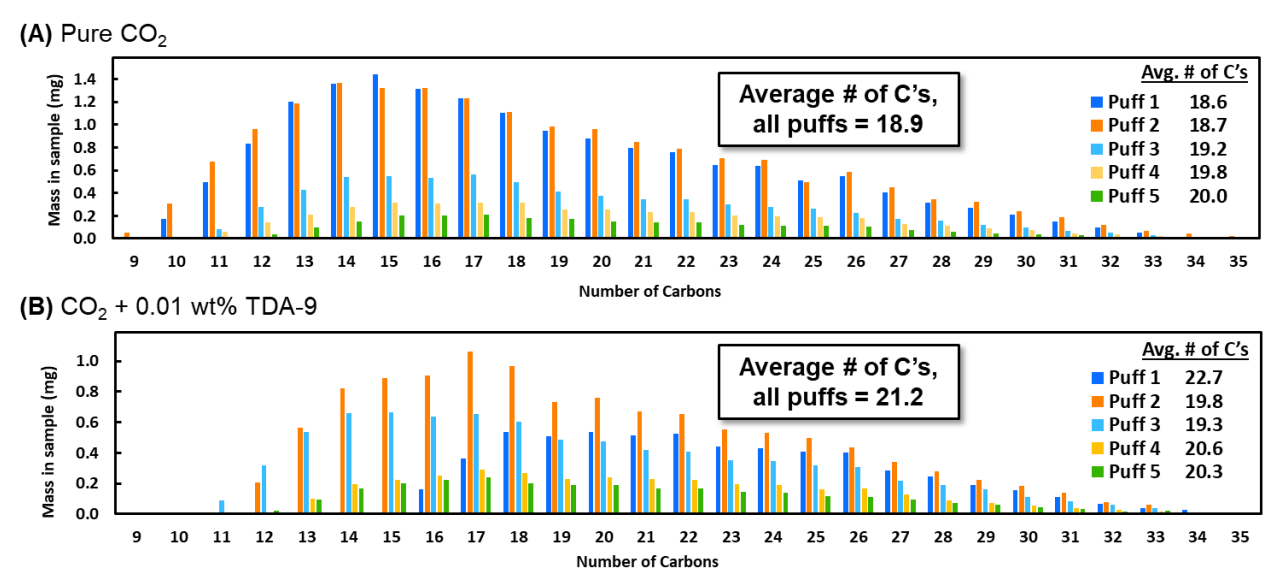


Figure 13. GC-MS analysis of hydrocarbons produced during confined huff-n-puff experiments. Light hydrocarbons are expected to dissipate with the CO₂ phase and are not included in this analysis. The average number of carbons for all puffs is weighted by the incremental recovery of each puff.

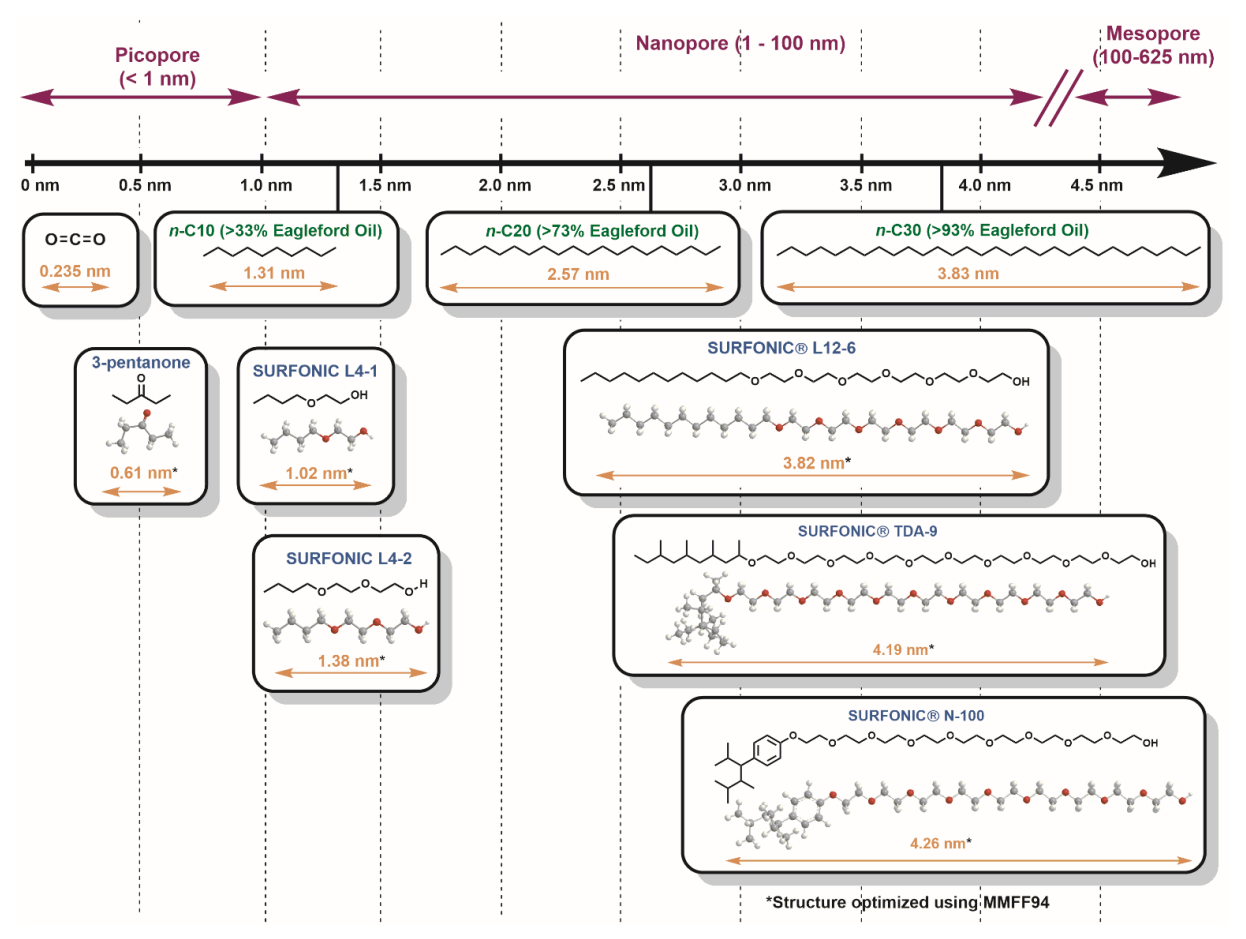


Figure 14. Comparison of surfactant and hydrocarbon sizes with shale pores. Surfactant structures were optimized in the gas phase with MMFF94 energy minimization using ChemDraw 3D 17.1.

4. CONCLUSION

This work represents first steps toward improving CO₂ EOR by adding surfactants dissolved in CO₂ to change the shale reservoir from oil-wet to water-wet. We have

demonstrated several important criteria necessary for CO₂-dissolved surfactants to be considered as a viable EOR technique for shale reservoirs. First, we found that CO₂ and oil are not completely miscible at reservoir conditions. Therefore, although CO₂ is already a good EOR fluid for

conventional reservoirs, it can be further improved for application in shale reservoirs, where multi-contact miscibility is not achieved, through the addition of surfactants. Secondly, we showed that nonionic CO₂-soluble surfactants are capable of altering shale wettability from oil-wet to CO₂-oil intermediate-wet. Because no change in CO₂-oil IFT was observed upon addition of surfactant, and no foam was generated by the surfactant, the most likely mechanism of oil recovery by nonionic CO₂-dissolved surfactants is wettability alteration. Initial huff-n-puff experiments showed that CO2 solutions of SURFONIC® TDA-9 (0.01 wt% and o.1 wt%) can improve oil recovery by several percentage points over CO2 alone. Analysis of produced hydrocarbons by GC-MS demonstrates the ability of the CO₂dissolved surfactant to recover a higher proportion of heavier oil in the first puffs than pure CO₂. The surfactants chosen for this study were inexpensive (\$1-3/pound), commercially-available, and used in dilute amounts (as low as 0.01 wt%). With further optimization of surfactant structures to improve oil recoveries, the addition of nonionic surfactants to CO2 is a viable strategy for improving CO2 EOR in unconventional formations.

AUTHOR INFORMATION

Corresponding Authors

*Angela Goodman – United States Department of Energy, National Energy Technology Laboratory, 626 Cochrans Mill Road, P.O. Box 10940, Pittsburgh, PA 15236, USA.

orcid.org/oooo-ooo3-3004-3303 Email: angela.goodman@netl.doe.gov

*Robert M. Enick – University of Pittsburgh, Department of Chemical and Petroleum Engineering, 940 Benedum Engineering Hall, Pittsburgh, PA 15261.

orcid.org/oooo-ooo3-1801-8033

Email: rme@pitt.edu

Author

Lauren C. Burrows – NETL Support Contractor, 626 Cochrans Mill Road, P.O. Box 10940, Pittsburgh, PA 15236, USA.

orcid.org/0000-0001-6107-3308

Foad Haeri – NETL Support Contractor, 626 Cochrans Mill Road, P.O. Box 10940, Pittsburgh, PA 15236, USA. orcid.org/0000-0001-9658-8432

Deepak Tapriyal – NETL Support Contractor, 626 Cochrans Mill Road, P.O. Box 10940, Pittsburgh, PA 15236, USA.

Sean Sanguinito – NETL Support Contractor, 626 Cochrans Mill Road, P.O. Box 10940, Pittsburgh, PA 15236, USA.

Parth G. Shah – University of Pittsburgh, Department of Chemical and Petroleum Engineering, 940 Benedum Engineering Hall, Pittsburgh, PA 15261.

Peter Lemaire – University of Pittsburgh, Department of Chemical and Petroleum Engineering, 940 Benedum Engineering Hall, Pittsburgh, PA 15261.

Dustin Crandall – United States Department of Energy, National Energy Technology Laboratory, 3610 Collins Ferry Rd, Morgantown, WV 26505, USA.

Funding Sources

This work was performed in support of the U.S. Department of Energy's Fossil Energy Crosscutting Technology Research Program. The Research was executed through the National Energy Technology Laboratory (NETL) Research and Innovation Center's Onshore Unconventional Resources Portfolio.

ACKNOWLEDGMENT

We would like to thank Dr. Luis Salazar of Indorama Oxides and Derivatives for many useful discussions and for providing samples of nonionic surfactants SURFONIC* TDA-9, N-100, and L12-6. We thank Eddie Bruner and Larry Robertson of Continental Resources, Inc. for supplying Eagle Ford crude oil samples.

NOTES

This project was funded by the United States Department of Energy, National Energy Technology Laboratory, in part, through a site support contract. Neither the United States Government nor any agency thereof, nor any of their employees, nor the support contractor, nor any of their employees, makes any warranty, express or implied, or assumes any legal liability or responsibility for the accuracy, completeness, or usefulness of any information, apparatus, product, or process disclosed, or represents that its use would not infringe privately owned rights. Reference herein to any specific commercial product, process, or service by trade name, trademark, manufacturer, or otherwise does not necessarily constitute or imply its endorsement, recommendation, or favoring by the United States Government or any agency thereof. The views and opinions of authors expressed herein do not necessarily state or reflect those of the United States Government or any agency thereof.

The authors declare no competing financial interest.

ABBREVIATIONS

C, carbon; CO₂, carbon dioxide; DCM, dichloromethane; EO, ethylene oxide; EOR, enhanced oil recovery; GC-MS, gas chromatography mass spectrometry; h, hour; IFT, interfacial tension; MMP, minimum miscibility pressure; mN/m, millinewtons per meter; MPa, megapascals; PEO, polyethylene oxide; PDMS, polydimethylsiloxane; PPO, polypropylene oxide; Px, pressure-composition; rpm, rotations per minute; rt, room temperature; SAG, surfactant-alternating gas.

REFERENCES

(1) EIA Annual Energy Outlook 2022. https://www.eia.gov. (2) The White House: Briefing Room, Statement and Releases. FACT SHEET: President Biden's Plan to Respond to Putin's Price Hike at the Pump. https://www.whitehouse.gov/briefing-room/statements-releases/2022/03/31/fact-sheet-president-bidens-plan-to-respond-to-putins-price-hike-at-the-pump/?utm_source=link">https://www.whitehouse.gov/briefing-room/statements-releases/2022/03/31/fact-sheet-president-bidens-plan-to-respond-to-putins-price-hike-at-the-pump/?utm_source=link">https://www.whitehouse.gov/briefing-room/statements-releases/2022/03/31/fact-sheet-president-bidens-plan-to-respond-to-putins-price-hike-at-the-pump/?utm_source=link (accessed May 16, 2022).

(3) Burrows, L. C.; Haeri, F.; Cvetic, P.; Sanguinito, S.; Shi, F; Tapriyal, D.; Goodman, A.; Enick, R. M., A Literature Review

- of CO₂, Natural Gas, and Water-Based Fluids for Enhanced Oil Recovery in Unconventional Reservoirs. *Energy Fuels* **2020**, *34*, 5331-5380.
- (4) Tang, W.; Sheng, J. J., Huff-n-puff Gas Injection or Gas Flooding in Tight Oil Reservoirs? *J. Pet. Sci. Eng.* **2022**, 208, 109725.
- (5) Qiao, R.; Li, F.; Zhang, S.; Wang, H.; Wang, F.; Zhou, T., CO₂ Mass Transfer and Oil Replacement Capacity in Fractured Shale Oil Reservoirs: From Laboratory to Field. *Frontiers in Earth Science* **2022**, *9*, 1-13.
- (6) Zhou, X.; Li, X.; Shen, D.; Shi, L.; Zhang, Z.; Sun, X.; Jiang, Q., CO₂ Huff-n-Puff Process to Enhance Heavy Oil Recovery and CO₂ Storage: An Integration Study. *Energy* **2022**, 239, 122003.
- (7) Li, S.; Sun, L.; Wang, L.; Li, Z.; Zhang, K., Hybrid CO₂-N₂ Huff-n-Puff Strategy in Unlocking Tight Oil Reservoirs. *Fuel* **2022**, 309, 122198.
- (8) Ma, N.; Li, C.; Wang, F.; Liu, Z.; Zhang, Y.; Jiang, L.; Shu, Y.; Du, D., Laboratory Study on the Oil Displacement Process in Low-Permeability Cores with Different Injection Fluids. *ACS Omega* 2022, 7, 8013-8022.
- (9) Badrouchi, N.; Pu, H.; Smith, S.; Badrouchi, F., Evaluation of CO₂ Enhanced Oil Recovery in Unconventional Reservoirs: Experimental Parametric Study in the Bakken. *Fuel* **2022**, *312*, 122041.
- (10) Hawthorne, S. B.; Grabanski, C. B.; Jin, L.; Bosshart, N. W.; Miller, D. J., Comparison of CO₂ and Produced Gas Hydrocarbons to Recover Crude Oil from Williston Basin Shale and Mudrock Cores at 10.3, 17.2, and 34.5 MPa and 110 °C. *Energy Fuels* **2021**, 35, 6658-6672.
- (11) Altawati, F.; Emadi, H.; Pathak, S., Improving Oil Recovery of Eagle Ford Shale Samples using Cryogenic and Cyclic Gas Injection Methods An Experimental Study. *Fuel* **2021**, 302, 121170.
- (12) Zhu, C.-F.; Guo, W.; Wang, Y.-P.; Li, Y.-J.; Gong, H.-J.; Xu, L.; Dong, M.-Z., Experimental Study of Enhanced Oil Recovery by CO₂ Huff-n-Puff in Shales and Tight Sandstones with Fractures. *Petroleum Science* **2021**, *18*, 852-869.
- (13) Tovar, F. D.; Barrufet, M. A.; Schechter, D. S., Enhanced Oil Recovery in the Wolfcamp Shale by Carbon Dioxide or Nitrogen Injection: An Experimental Investigation. *SPE J.* **2021**, *26*, 515-537.
- (14) Yue, P.; Zhang, R.; Sheng, J. J.; Yu, G.; Liu, F., Study on the Influential Factors of CO₂ Storage in Low Permeability Reservoir. *Energies* **2022**, *15*, 344-354.
- (15) Fakher, S.; Imqam, A., Application of Carbon Dioxide Injection in Shale Oil Reservoirs for Increasing Oil Recovery and Carbon Dioxide Storage. *Fuel* **2020**, *265*, 116944.
- (16) Peck, W. D.; Ayash, S. C.; Klapperich, R. J.; Gorecki, C. D., The North Dakota Integrated Carbon Storage Complex Feasibility Study. *Int. J. Greenhouse Gas Control* **2019**, *84*, 47-53.
- (17) Peck, W. D.; Azzolina, N. A.; Ge, J.; Bosshart, N. W.; Burton-Kelly, M. E.; Gorecki, C. D.; Gorz, A. J.; Ayash, S. C.; Nakles, D. V.; Melzer, L. S., Quantifying CO₂ Storage Efficiency Factors in Hydrocarbon Reservoirs: A Detailed Look at CO₂ Enhanced Oil Recovery. *Int. J. Greenhouse Gas Control* **2018**, *69*, 41-51.
- (18) Jin, L.; Pekot, L. J.; Smith, S. A.; Salako, O.; Peterson, K. J.; Bosshart, N. W.; Hamling, J. A.; Mibeck, B. A. F.; Hurley, J. P.; Beddoe, C. J.; Gorecki, C. D., Effects of Gas Relative Permeability Hysteresis and Solubility on Associated CO₂ Storage Performance. *Int. J. Greenhouse Gas Control* **2018**, 75, 140-150.

- (19) Azzolina, N. A.; Peck, W. D.; Hamling, J. A.; Gorecki, C. D.; Ayash, S. C.; Doll, T. E.; Nakles, D. V.; Melzer, L. S., How Green is my Oil? A Detailed Look at Greenhouse Gas Accounting for CO₂-Enhanced Oil Recovery (CO₂-EOR) Sites. *Int. J. Greenhouse Gas Control* **2016**, *51*, 369-379.
- (20) Burrows, L. C.; Haeri, F.; Tapriyal, D.; Lemaire, P.; Shah, P. G.; Alenzi, A.; Enick, R. M.; Crandall, D. M.; Goodman, A. In *CO₂-Soluble Surfactants for Enhanced Oil Recovery from Shale*, SPE/AAPG/SEG Unconventional Resources Technology Conference, 2021.
- (21) Haeri, F.; Burrows, L.; Lemaire, P.; Alenzi, A.; Shah, P.; Tapriyal, D.; Enick, R.; Crandall, D.; Goodman, A. In Laboratory-Scale CO₂ Huff 'n Puff EOR using Single Phase Solutions of CO₂ and CO₂ Soluble, Nonionic, Wettability Altering Additives, SPE Annual Technical Conference and Exhibition, 2020.
- (22) Haeri, F.; Burrows, L. C.; Lemaire, P.; Shah, P. G.; Tapriyal, D.; Enick, R. M.; Crandall, D. M.; Goodman, A. In *Improving CO₂-EOR In Shale Reservoirs using Dilute Concentrations of Wettability-Altering CO₂-Soluble Nonionic Surfactants*, SPE/AAPG/SEG Unconventional Resources Technology Conference, 2020.
- (23) Omari, A.; Cao, R.; Zhu, Z.; Xu, X., A Comprehensive Review of Recent Advances on Surfactant Architectures and their Applications for Unconventional Reservoirs. *J. Pet. Sci. Eng.* 2021, 206, 109025.
- (24) Sheng, J. J., Chapter Nine EOR Mechanisms of Wettability Alteration and its Comparison with IFT. In *Enhanced Oil Recovery in Shale and Tight Reservoirs*, Sheng, J. J., Ed. Gulf Professional Publishing: 2020; pp 213-278.
- (25) Some specialty florinated or oxygenated ionic surfactants are soluble in CO₂, but due to their enviornmental toxicity and cost, they would not be appropriate for this application. Eastoe, J.; Gold, S.; Steytler, D. C., Surfactants for CO₂. Langmuir 2006, 22, 9832–9842.
- (26) Jian, G.; Fernandez, C. A.; Puerto, M.; Sarathi, R.;Bonneville, A.; Biswal, S. L., Advances and Challenges in CO₂ Foam Technologies for Enhanced Oil Recovery in Carbonate Reservoirs. *J. Pet. Sci. Eng.* **2021**, 202, 108447.
- (27) McLendon, W. J.; Koronaios, P.; Enick, R. M.; Biesmans, G.; Salazar, L.; Miller, A.; Soong, Y.; McLendon, T.; Romanov, V.; Crandall, D., Assessment of CO₂-Soluble Non-Ionic Surfactants for Mobility Reduction using Mobility Measurements and CT Imaging. *J. Pet. Sci. Eng.* **2014**, *119*, 196-209.
- (28) McLendon, W. J.; Koronaios, P.; McNulty, S.; Enick, R. M.; Biesmans, G.; Miller, A. N.; Salazar, L. C.; Soong, Y.; Romanov, V.; Crandall, D., Assessment of CO₂-Soluble Surfactants for Mobility Reduction using Mobility Measurements and CT Imaging. In *SPE Improved Oil Recovery Symposium*, Society of Petroleum Engineers: Tulsa, Oklahoma, USA, 2012; p 26.
- (29) Sanders, A. W.; Jones, R. M.; Linroth, M. A.; Nguyen, Q. P., Implementation of a CO₂ Foam Pilot Study in the SACROC Field: Performance Evaluation. In *SPE Annual Technical Conference and Exhibition*, Society of Petroleum Engineers: San Antonio, Texas, USA, **2012**; p 13.
- (30) Ren, G.; Zhang, H.; Nguyen, Q. P., Effect of Surfactant Partitioning Between CO₂ and Water on CO₂ Mobility Control in Hydrocarbon Reservoirs. In *SPE Enhanced Oil Recovery Conference*, Society of Petroleum Engineers: Kuala Lumpur, Malaysia, **2011**; p 15.
- (31) Sanders, A.; Nguyen, Q. P.; Nguyen, N.; Adkins, S.; Johnston, K. P., Twin-Tailed Surfactants for Creating CO₂-in-Water Macroemulsions for Sweep Enhancement in CO₂-EOR.

- In *Abu Dhabi International Petroleum Exhibition and Conference*, Society of Petroleum Engineers: Abu Dhabi, UAE, **2010**; p. 8.
- (32) Le, V. Q.; Nguyen, Q. P.; Sanders, A., A Novel Foam Concept With CO₂ Dissolved Surfactants. In *SPE Symposium* on *Improved Oil Recovery*, Society of Petroleum Engineers: Tulsa, Oklahoma, USA, **2008**; p 15.
- (33) Chen, W.; Schechter, D. S., Surfactant Selection for Enhanced Oil Recovery Based on Surfactant Molecular Structure in Unconventional Liquid Reservoirs. *J. Pet. Sci. Eng.* **2021**, *196*, 107702.
- (34) Gajbhiye, R., Effect of CO_2/N_2 Mixture Composition on Interfacial Tension of Crude Oil. *ACS Omega* **2020**, 5, 27944-27952.
- (35) Hemmati-Sarapardeh, A.; Ayatollahi, S.; Ghazanfari, M.-H.; Masihi, M., Experimental Determination of Interfacial Tension and Miscibility of the CO₂–Crude Oil System; Temperature, Pressure, and Composition Effects. *J. Chem. Eng. Data* **2014**, *59*, 61-69.
- (36) Rezk, M. G.; Foroozesh, J., Phase Behavior and Fluid Interactions of a CO₂-Light Oil System at High Pressures and Temperatures. *Heliyon* **2019**, 5, e02057.
- (37) Qian, K.; Yang, S.; Dou, H.; Wang, Q.; Wang, L.; Huang, Y., Experimental Investigation on Microscopic Residual Oil Distribution During CO₂ Huff-and-Puff Process in Tight Oil Reservoirs. *Energies* **2018**, *11*, 1-16.
- (38) Alzobaidi, S.; Angeles, T.; Rodriguez, G.; Johnston, K. P.; Enick, R. M., Carbon Dioxide-in-Oil (C/O) Emulsions Stabilized by Silica Nanoparticles Functionalized with Oleophilic and CO₂-philic Ligands. *Ind. Eng. Chem. Res.* **2022**, 12092-12106.
- (39) Alzobaidi, S.; Lee, J.; Jiries, S.; Da, C.; Harris, J.; Keene, K.; Rodriguez, G.; Beckman, E.; Perry, R.; Johnston, K. P.; Enick, R., Carbon Dioxide-in-Oil Emulsions Stabilized with Silicone-Alkyl Surfactants for Waterless Hydraulic Fracturing. *J. Colloid Interface Sci.* 2018, 526, 253-267.
- (40) Saputra, I. W. R.; Adebisi, O.; Ladan, E. B.; Bagareddy, A.; Sarmah, A.; Schechter, D. S., The Influence of Oil Composition, Rock Mineralogy, Aging Time, and Brine Pre-Soak on Shale Wettability. *ACS Omega* **2022**, *7*, 85-100.
- (41) Wang, Y.; Xu, H.; Yu, W.; Bai, B.; Song, X.; Zhang, J., Surfactant Induced Reservoir Wettability Alteration: Recent Theoretical and Experimental Advances in Enhanced Oil Recovery. *Petroleum Science* **2011**, *8*, 463-476.
- (42) Buckley, J. S.; Liu, Y.; Monsterleet, S., Mechanisms of Wetting Alteration by Crude Oils. *SPE J.* **1998**, 3, 54-61.
- (43) Although there have been many prior studies of adsorption of compounds from solution in CO2 onto solid surfaces, the objectives of these studies were related to separation techniques, fluid purification processes, and deposition of chemical species within nanostructure frameworks, rather than the alteration of wettability.
- (44) Bozbağ, S. E.; Erkey, C., Supercritical Deposition: Current Status and Perspectives for the Preparation of Supported Metal Nanostructures. *J. Supercrit. Fluids* **2015**, *96*, 298-312.
- (45) Tenorio, M. J.; Cabañas, A.; Pando, C.; Renuncio, J. A. R., Solubility of Pd(hfac)₂ and Ni(hfac)₂·2H₂O in Supercritical Carbon Dioxide Pure and Modified with Ethanol. *J. Supercrit. Fluids* **2012**, 70, 106-111.
- (46) Xing, H.; Su, B.; Ren, Q.; Yang, Y., Adsorption Equilibria of Artemisinin from Supercritical Carbon Dioxide on Silica Gel. *J. Supercrit. Fluids* **2009**, *49*, 189-195.
- (47) Lübbert, M.; Brunner, G.; Johannsen, M., Adsorption Equilibria of α and δ -Tocopherol from Supercritical Mixtures of Carbon Dioxide and 2-Propanol onto Silica by Means of

- Perturbation Chromatography. J. Supercrit. Fluids 2007, 42, 180-188.
- (48) Brunner, G.; Johannsen, M., New Aspects on Adsorption from Supercritical Fluid Phases. *J. Supercrit. Fluids* **2006**, *38*, 181-200.
- (49) Zhang, F.; Adel, I. A.; Park, K. H.; Saputra, I. W. R.; Schechter, D. S., Enhanced Oil Recovery in Unconventional Liquid Reservoir Using a Combination of CO₂ Huff-n-Puff and Surfactant-Assisted Spontaneous Imbibition. In *SPE Annual Technical Conference and Exhibition*, Society of Petroleum Engineers: Dallas, Texas, USA, 2018; p 20.
- (50) Wei, J.; Zhou, X.; Zhou, J.; Li, J.; Wang, A., CO₂ Huff-n-Puff after Surfactant-Assisted Imbibition to Enhance Oil Recovery for Tight Oil Reservoirs. *Energy Fuels* **2020**, *34*, 7058-7066.
- (51) Zeng, T.; Miller, C. S.; Mohanty, K. K., Combination of a Chemical Blend with CO₂ Huff-n-Puff for Enhanced Oil Recovery in Oil Shales. *J. Pet. Sci. Eng.* **2020**, *194*, 107546.
- (52) Zhang, F.; Schechter, D. S., Gas and Foam Injection with CO₂ and Enriched NGL's for Enhanced Oil Recovery in Unconventional Liquid Reservoirs. *J. Pet. Sci. Eng.* **2021**, 202, 108472.
- (53) Zhang, C.; Xi, L.; Wu, P.; Li, Z., A Novel System for Reducing CO₂-Crude Oil Minimum Miscibility Pressure with CO₂-Soluble Surfactants. *Fuel* **2020**, *281*, 118690.
- (54) Ding, M.; Wang, Y.; Wang, W.; Zhao, H.; Liu, D.; Gao, M., Potential to Enhance CO₂ Flooding in Low Permeability Reservoirs by Alcohol and Surfactant as Co-Solvents. *J. Pet. Sci. Eng.* **2019**, *182*, 106305.
- (55) Zhang, C.; Li, Z.; Li, S.; Lv, Q.; Wang, P.; Liu, J.; Liu, J., Enhancing Sodium Bis(2-ethylhexyl) Sulfosuccinate Injectivity for CO₂ Foam Formation in Low-Permeability Cores: Dissolving in CO₂ with Ethanol. *Energy Fuels* **2018**, 32, 5846-5856.
- (56) Luo, H.; Zhang, Y.; Fan, W.; Nan, G.; Li, Z., Effects of the Non-ionic Surfactant (C_iPO_j) on the Interfacial Tension Behavior between CO_2 and Crude Oil. *Energy Fuels* **2018**, 32, 6708-6712.
- (57) Cimadom, D.; Moore, J.; Paronish, T.; Schmitt, R.; Sanguinito, S.; Crandall, D.; Dotson, B. *Core Characterization of Bakken Shale from the Bedwell* 33-52-1-1H *Well, Sheridan County, Montana*; U.S. Department of Energy, National Energy Technology Laboratory: 2021.
- (58) A single test was conducted in which a shale chip was soaked in 3.5% NaCl brine for one week, followed by soaking in oil (80 °C) for one week; the contact angle of water on the oil-soaked chip was 99°, slightly less than the 117 ± 5 ° result without brine soak. The shale surface was still rendered intermediate-wet, albeit not as strongly oil-wet as the shale chip soaked in oil alone.
- (59) Fan, Xin; Potluri, V. K.; McLeod, M. C.; Wang, Y.; Liu, J.; Enick, R. M.; Hamilton, A. D.; Roberts, C. B.; Johnson, J. K.; Beckman, E. J., Oxygenated Hydrocarbon Ionic Surfactants Exhibit CO₂ Solubility. *J. Am. Chem. Soc.* **2005**, *127*, 11754-11762. (60) Lu, J.; Darvari, R.; Nicot, J.-P.; Mickler, P.; Hosseini, S. A., Geochemical Impact of Injection of Eagle Ford Brine on Hosston Sandstone Formation—Observations of Autoclave Water–Rock Interaction Experiments. *Appl. Geochem.* **2017**, *84*, 26-40.
- (61) Jaeger, P. Interfacial Tension under Non-Standard Pressure Conditions; Krűss: 2003.
- (62) Haeri, F.; Tapriyal, D.; Sanguinito, S.; Shi, F.; Fuchs, S. J.; Dalton, L. E.; Baltrus, J.; Howard, B.; Crandall, D.; Matranga, C.; Goodman, A., CO₂–Brine Contact Angle Measurements on

- Navajo, Nugget, Bentheimer, Bandera Brown, Berea, and Mt. Simon Sandstones. *Energy Fuels* **2020**, 34, 6085-6100.
- (63) Hawthorne, S. B.; Miller, D. J.; Grabanski, C. B.; Azzolina, N.; Kurz, B. A.; Ardakani, O. H.; Smith, S. A.; Sanei, H.; Sorensen, J. A., Hydrocarbon Recovery from Williston Basin Shale and Mudrock Cores with Supercritical CO₂: Part 1. Method Validation and Recoveries from Cores Collected across the Basin. *Energy Fuels* **2019**, 33, 6857-6866.
- (64) The position of the nearly vertical cloud point curve on the right-hand side of this figure was not determined, its position in the figure close to 100% CO₂ is qualitative; there is a narrow single-phase region to the right of the cloud point curve and the wt.% CO₂ = 100% vertical axis, but the position of this particular locus is not practical to determine using the technique described in this paper.
- (65) Pollack, N. R.; Enick, R. M.; Mangone, D. J.; Morsl, B. I., Effect of an Aqueous Phase on CO₂/Tetradecane and CO₂/Maljamar-Crude-Oil Systems. *SPE Reservoir Eng.* 1988, 3, 533-541.
- (66) Orr, F. M., Jr.; Jensen, C. M., Interpretation of Pressure-Composition Phase Diagrams for CO₂/Crude-Oil Systems. *Soc. Pet. Eng. J.* **1984**, 24, 485-497.
- (67) Xiong, Y. Development of a Compositional Model Fully Coupled with Geomechanics and its Application to Tight Oil Reservoir Simulation. PhD Thesis, Colorado School of Mines, Golden, Colorado, 2015.
- (68) Isotherms were not measured at 80 °C because these measurements were made during the early stages of the project, before the temperature was selected for the CO₂-oil phase behavior experiments and the CO₂ huff-n-puff tests.
- (69) Xing, D., Wei, B.; McLendon, W.; Enick, R.; McNulty, S.; Trickeff, K.; Mohamed, A.; Cummings, S.; Eastoe, J.; Rogers, S.; Crandall, D.; Tennant, B.; McLendon, T.; Romanov, V.; Soong, Y., CO₂-Soluble, Nonionic, Water-Soluble Surfactants That Stabilize CO₂-in-Brine Foams. *SPE J.* **2012**, *17*, 1172-1185.

- (70) Schön, J. H., Chapter 2 Pore Space Properties. In *Developments in Petroleum Science*, Schön, J. H., Ed. Elsevier: 2015; Vol. 65, pp 21-84.
- (71) Alharthy, N.; Teklu, T.; Kazemi, H.; Graves, R.; Hawthorne, S.; Braunberger, J.; Kurtoglu, B., Enhanced Oil Recovery in Liquid–Rich Shale Reservoirs: Laboratory to Field. *SPE Reservoir Eval. Eng.* **2017**, *21*, 137–159.
- (72) Alzobaidi, S.; Lee, J.; Jiries, S.; Da, C.; Harris, J.; Keene, K.; Rodriguez, G.; Beckman, E.; Perry, R.; Johnston, K. P.; Enick, R., Carbon Dioxide-in-Oil Emulsions Stabilized with Silicone-Alkyl Surfactants for Waterless Hydraulic Fracturing. *J. Colloid Interface Sci.* 2018, 526, 253-267.
- (73) Our only success in generating CO₂-in-oil emulsions and foams was realized using specialty oil-soluble PDMS-triacontane copolymers or oil-dispersible silica nanoparticles surface-functionalized with hexadecane and ethyl acetate ligands.
- (74) Zeng, T.; Kim, K. T.; Werth, C. J.; Katz, L. E.; Mohanty, K. K., Surfactant Adsorption on Shale Samples: Experiments and an Additive Model. *Energy Fuels* **2020**, 34, 5436-5443.
- (75) Wang, M.; Abeykoon, G. A.; Argüelles-Vivas, F. J.; Okuno, R., Aqueous Solution of 3-Pentanone for Enhanced Oil Production from Tight Porous Media. *J. Pet. Sci. Eng.* 2022, 213, 110376.
- (76) Wang, M.; Abeykoon, G. A.; Argüelles-Vivas, F. J.; Okuno, R., Aqueous Solution of Ketone Solvent for Enhanced Water Imbibition in Fractured Carbonate Reservoirs. *SPE J.* **2020**, *25*, 2694-2709.
- (77) Zhang, Z.; Pan, S.-Y.; Li, H.; Cai, J.; Olabi, A. G.; Anthony, E. J.; Manovic, V., Recent Advances in Carbon Dioxide Utilization. *Renewable Sustainable Energy Rev.* **2020**, *125*, 109799.

